Atmos. Chem. Phys. Discuss., https://doi.org/10.5194/acp-2018-948
Manuscript under review for journal Atmos. Chem. Phys.
Discussion started: 1 October 2018
© Author(s) 2018. CC BY 4.0 License.

Atmospheric Chemistry and Physics Discussions

Country-scale greenhouse gases budgets using shipborne measurements: a case study for the United Kingdom and Ireland.

Carole Helfter[1], Neil Mullinger[1], Massimo Vieno[1], Simon O'Doherty[2], Michel Ramonet[3], Paul I. Palmer[4] and Eiko Nemitz[1].

[1]Centre for Ecology and Hydrology, Penicuik, UK
[2]School of Chemistry, University of Bristol, UK
[3]Laboratoire des Sciences du Climat et de l'Environnement, CEA-CNRS-UVSQ, Gif-sur-Yvette, France
[4]School of GeoSciences, University of Edinburgh, Edinburgh, UK

Correspondence to: Carole Helfter (caro2@ceh.ac.uk)

Abstract. We present a mass balance approach to estimate the seasonal and annual budgets of carbon dioxide (CO_2) and methane (CH_4) of the United Kingdom (excluding Scotland) and the Republic of Ireland from concentration measurements taken on a ferry along the east coast of the United Kingdom over a 3-year period (2015-2017). We estimate the annual emissions of CH_4 to be 2.55 ± 0.43 Tg, which is consistent with the combined 2.29 Tg reported to the United Nations Framework Convention on Climate Change by the individual countries. The net CO_2 budget (i.e. including all anthropogenic and biogenic sources and sinks of CO_2) is estimated at 881.0 ± 137.5 Tg, with a net biogenic contribution of 458.7 Tg (taken as the difference between the estimated net emissions and the inventory value which accounts for anthropogenic emissions only). The largest emissions for both gases were observed in a broad latitudinal band (52.5 °N – 54 °N), which coincides with densely populated areas. The emissions of both gases were seasonal (maxima in winter and minima in summer), strongly correlated to natural gas usage and, to a lesser extent, also anti-correlated to mean air temperature. Methane emissions exhibited a statistically significant anti-correlation with air temperature at the seasonal time scale in the central region spanning 52.8 °N – 54.2 °N, which hosts a relatively high density of waste treatment facilities. Methane emissions from landfills have been shown to sometimes increase with decreasing air temperature due to changes in the CH_4-oxidizing potential of the top soil, and we speculate that the waste sector contributes significantly to the CH_4 budget of this central region. This study brings independent verification of the emission budgets estimated using alternative products (e.g. mass balance budgets by aircraft measurements, inverse modelling, inventorying) and offers an opportunity to investigate the seasonality of these emissions which is usually not possible.

1 Introduction

The United Nations Framework Convention on Climate Change (UNFCCC), kick-started an international political drive to reduce emissions of greenhouse gases (GHG) and stabilise their mid- to long-term impact on the global climate. The focus of the international community over the past 2-3 decades has been on curbing emissions of carbon dioxide (CO_2), the most abundant and well-understood GHG, but it is now recognised that emissions of other GHGs such as methane (CH_4) and nitrous oxide (N_2O) must also be addressed in order to fulfil the goal of limiting irreversible climate change set out under the 21st Convention of Parties (COP21). Reductions in CH_4 emissions in particular would be effective in reducing GHGs more quickly, given its shorter lifetime. Annex 1 parties are required to report their GHG inventories annually to the UNFCCC following the guidelines set out by the Intergovernmental Panel on Climate Change (IPCC, 2006; UNFCCC, 2014). Emissions inventories are powerful tools but they intrinsically rely on detailed knowledge of source abundance and strength and they can therefore carry significant uncertainties. For example, uncertainties on the fossil fuel emissions from Europe and North America have been estimated to be of the order of 2% to 5% (Marland, 2012); in contrast, a 1.4 Gt gap in CO_2 emissions was reported in China in 2010, which was equivalent to ~ 5% of the global budget (Guan et al., 2012). Because much of its emission is directly

© Author(s) 2018. CC BY 4.0 License.

linked to the amount of fossil fuel used, CO_2 is the best-understood GHG but, despite this, regional and consequently global emissions budgets are thought to be under-estimated and the uncertainties are increasing due to the growing emissions from emerging economies (Gregg et al., 2008; Gregg, 2008; Peters et al., 2011). By contrast, relatively more of the CH_4 emission is mediated by biological processes. After a period of stagnation in the first few years of the 21st century, atmospheric CH_4 has been rising steadily since ca. 2007. This prompted renewed efforts by the international scientific community to identify the drivers of CH_4 at local, regional and global scales and reconcile bottom-up and top-down estimates (Kirschke et al., 2013; Saunois et al., 2016). At the global scale, total methane emissions from fossil fuels (from the fossil fuel industry and from geological seepage) have been relatively steady over the past three decades but research indicates that the estimates must be revised upwards by as much as 60%-110% (Schwietzke et al., 2016). The recent rise in atmospheric methane has been attributed to increases in emissions from microbial sources, which are meteorologically driven and can therefore exhibit substantial inter-annual variability (Dlugokencky et al., 2011; Schwietzke et al., 2016). Inventories are thought to over-estimate global emissions and a difference of 130 Tg CH_4 y^{-1} was found between bottom-up and top-down estimates (Kirschke et al., 2013). In this light, it is becoming increasingly clear that there is an urgent need to seek independent validation of the emissions inventories using an integrated range of measurements and modelling activities (Allen, 2016; Nisbet and Weiss, 2010).

The development in recent years of rugged, high-precision spectroscopic instruments (e.g. Peltola et al., 2014) has opened up new opportunities for continuous, in-situ measurements of methane at fine temporal resolution and at relatively large spatial scales. For example, such sensors have been used in airborne applications to study methane emissions from cities (Cambaliza et al., 2015; Cambaliza et al., 2014; Mays et al., 2009; O'Shea et al., 2014) as well as anthropogenic and biogenic area sources (Hiller et al., 2014; Karion et al., 2015; Karion et al., 2013). Applications of eddy-covariance to measure emission / deposition directly at the field scale are on the rise in a broad variety of environments ranging from agricultural and wetlands (Dengel et al., 2011; Erkkila et al., 2018; Felber et al., 2015; Meijide et al., 2011; Peltola et al., 2015; Podgrajsek et al., 2014; Nicolini et al., 2013) to urban (Gioli et al., 2012; Helfter et al., 2011; Helfter et al., 2016; Pawlak and Fortuniak, 2016; Pawlak et al., 2016). Finally, networks of tall towers and networks thereof exist around the world to monitor and model methane emissions at spatial scales ranging from country to global (Bakwin et al., 1995; Bohnenstengel et al., 2015; Feng et al., 2009; Feng et al., 2011; Miller et al., 2013; Oney et al., 2015; Rigby et al., 2008; Stanley et al., 2018; Stavert et al., 2018).

The geography of the British Isles at the NE edge of Europe, with dominantly SW winds advecting clean Atlantic air masses, particularly lends itself to a further approach, namely boundary layer budget measurements of the concentrations in the in- and outflow. This has previously been utilised for airborne boundary layer budget measurements (Fowler et al., 1996; Gallagher et al., 1994; Polson et al., 2011), but these can only provide snapshots of the country emissions for a few individual days.

Extending the concept of these earlier studies, we present three years of continuous observations (2015-2017) of CO_2 and CH_4 concentrations measured on-board a commercial freight ferry, which connects the ports of Rosyth (Scotland, UK) to Zeebrugge (Belgium) and tracks the East Coast of most of Great Britain. The route of the ferry transects the UK outflow with a time-dependent footprint (Fig. 1), which, combined with typical West-to-East air mass travel time of 11 to 19 hours across the domain (median values for winter and summer, respectively) allows for sub-daily emissions estimations. Furthermore, the three continuous years of measurements also provide an opportunity to study seasonal and inter-annual changes in emissions. This is to our knowledge the first example of country-scale emission budgets using a mobile platform measuring continuously over several years.

These shipborne measurements formed part of a larger observation and modelling program - the Greenhouse gAs Uk and Global Emissions (GAUGE) project (Palmer et al., 2018) - aimed at determining the magnitude, spatial distribution and uncertainties of the UK's GHG budgets of CO_2, CH_4 and N_2O. In this paper we utilise shipborne observations at the outflow

© Author(s) 2018. CC BY 4.0 License.

of the United Kingdom coupled with background measurements at the Mace Head site (Ireland) to estimate seasonal and annual budgets of CO_2 and CH_4 using a mass balance approach.

2. Materials and methods

This section describes the measurement systems used at the two experimental sites (Mace Head and ferry) and provides details of the greenhouse gas budget calculations and mass balance approach.

2.1 Experimental setup

2.1.1 Shipborne measurements

Measurements of concentrations of carbon dioxide (CO_2) and methane (CH_4) began in February 2014 on board a commercial freight ferry (operated by DFDS Seaways) which served the route between Rosyth (Scotland, UK; 56° 1' 21.611'' N, 3° 26' 21.558'' W) and Zeebrugge (Belgium; 51° 21' 16.96'' N, 3° 10' 34.645'' E). The route of the ship followed the outline of the English coast on the East side of the UK, which placed it downwind of Atlantic air masses blowing in from the West over Ireland, Wales and England (Fig. 2). The ship completed three return journeys per week and typically operated for 48 weeks per calendar year. The schedule of the weekly cruises allowed for the latitude range to be sampled at different times of day and night as illustrated in Fig.3.

The roll-on/roll-off (Ro-Ro) cargo / container carrier vessel Finnmerchant (former name Longstone; IMO: 9234082; overall length and breadth: 193 m x 26 m) served the Rosyth – Zeebrugge route during the measurement period 25/02/2014 – 15/04/2014. It was replaced by the Ro-Ro cargo ship Finlandia Seaways (IMO: 9198721; overall length and breadth: 163 m x 21 m) on 15/06/2014 and measurement restarted aboard the new vessel.

Air was sampled on the topmost platform of the bow (port side on Finnmerchant and starboard side on Finlandia Seaways) and analysed by a cavity ring-down spectrometer (CRDS; Picarro 1301) housed in an air-conditioned measurement container located on the weather deck. Air was pumped at ca. 50 lpm through 20 m and 50 m of ½'' Synflex tubing at approximate measurement heights 20 m and 30 m a.s.l. (on Finnmerchant and Finlandia Seaways, respectively) and sub-sampled at ca. 10 lpm through 2 m of ¼'' Synflex tube by a secondary pump. The sub-sampling tee-piece was set up as a virtual impactor to prevent moisture and sea salt from entering the CRDS sampling line and the main sampling line was protected from moisture ingress by three water traps arranged in series (at the ambient air inlet point as well as immediately upstream and downstream of the virtual impactor).

The gas measurement system was equipped with a bespoke auto-calibration system controlled by an in-house LabView™ program which also handled the acquisition of data (0.5 Hz) from the Picarro gas analyser, a weather station (WXT520, Vaisala) co-located with the air inlet on the ship's top deck and a GPS (18x series, Garmin) receiver affixed to the roof of the sea container. Table 1 provides a list of observables and Table 2 summarises the weekly auto-calibration procedure.

2.1.2 Mace Head site

The Mace Head station is located on the west coast of Ireland at 53°20'N, 9 °54'W, 5 m above sea level, and a 23 m-high tower is used to sample the air. Atmospheric concentrations of CO_2 have been continuously monitored at Mace Head since 1992 (Biraud et al., 2000; Derwent et al., 2002; Ramonet et al., 2010). Since 2010 a cavity ring-down spectrometer similar to the one used on board the ship (Picarro, G1301), has been used for CO_2 and CH_4 measurements (instrument owned by the Environment Protection Agency (EPA), Ireland). A second CRDS analyser (Picarro, G2301) was installed in 2013 (instrument owned by Laboratoire des Sciences du Climat et de l'Environnement (LSCE), France), to ensure redundancy of measurements, thus reducing data gaps. Both analysers are calibrated simultaneously every month using a suite of four calibration cylinders whose concentrations span the atmospheric range. Those cylinders have themselves been calibrated at LSCE with

© Author(s) 2018. CC BY 4.0 License.

WMO/NOAA reference scales (WMO2007 scale for CO_2, WMO2004A scale for CH_4). In addition to the calibration cylinders, two target cylinders are regularly analysed (short-term target twice a day and long-term target once a month) in order to assess the measurements' repeatability. Over the period 2014-2018 the difference between the assigned values and the values measured every month at Mace Head for the long-term target gas were 0.01 ± 0.02 ppm for CO_2 (both analysers) and 0.08 ± 0.19 ppb and 0.01 ± 0.17 ppb for CH_4 with analyser G1301 and G2301 respectively. The measurements are processed every day at LSCE (Hazan et al., 2016), ensuring a high level of quality control of the dataset. The maintenance of the analysers is coordinated through close collaboration between LSCE, EPA and the National University of Ireland, Galway (NUIG).

2.2 Mass balance budgets

The main underlying assumptions of the mass balance approach used to calculate the spatially-integrated emissions budgets of CO_2 and CH_4 from the Republic of Ireland, Northern Ireland, Wales and England are five-fold:

- Under westerly wind conditions, the Mace Head station on the West coast of Ireland (53° 20' N, 9° 54' W; 5 m as.l., tower height 23 m) receives relatively clean Atlantic air, whilst the concentrations measured along the ferry route result from enhancement in CH_4 and CO_2 due to land sources over the travel path of the air mass. The concentrations at Mace Head are representative of the inflow into the British Isles in both space and time.

For each nominal temporal averaging period we assume that:

- The planetary boundary layer (PBL) height is constant over the entire spatial domain bounded to the East and West by the ferry route and the meridian at the Mace Head station location, respectively. The North and South boundaries of the domain are taken as the extrema of the latitudinal range covered by the ferry route.
- The air columns between the land surface and the top of the PBL are well-mixed.
- The horizontal wind direction is uniform.
- There is no mass leakage out of / or ingress into the 3D domain.

In the analysis, conditions are selected to fulfil these assumptions as best as possible. The estimation of background concentrations (baselines) and of the PBL height are presented in Sections 2.2.1 - 2.2.2; mass balance budget calculations and data quality control are discussed in Sections 2.2.3 - 2.2.4.

2.2.1 Data screening

Prior to time averaging and flux calculation, raw data points were excluded from further processing if any of the following criteria were realised:

- The ship was in port.
- A calibration took place.
- 72-hour back-trajectories for the Mace Head site and one point along route of the ferry (54.548 °N, 0.233 °W) as calculated with HYSPLIT (NOAA Air Resources Laboratory, 2018) exhibited air flow patterns inconsistent with the mass balance assumptions (i.e. non-westerly flow, evidence of re-circulation).
- The wind direction measured on the ship (absolute direction from North, corrected for the movement of the ship) was outside the Westerly range (240° - 300°).
- The wind direction measured at the Mace Head station (data source: Met Éireann, 2018) was outside the Westerly range (240° - 300°).

2.2.2 Concentration baselines

The time series of hourly concentrations of CO_2 and CH_4 measured at Mace Head and filtered for Westerly flow (wind direction range 240° – 300°) were used to construct continuous baselines for the measurement period February 2014 – December 2017

© Author(s) 2018. CC BY 4.0 License.

(Fig. 4). The time series of both gases exhibited well-defined seasonal cycles characterised by high concentrations towards the end of the winter and lower concentrations in summer. The baselines were constructed for the data period 01/01/2014 – 31/12/2017 by applying regressions by parts consisting of linear and non-linear (Gaussian) fitting functions over the temporal domain. The composite fitting functions provided smoothing and gap filling of the measured mole fractions time series and were subsequently used to construct continuous time series of background emissions of CO_2 and CH_4 with a 5-minute time step, which corresponded to the averaging interval used for the data measured on the ferry.

2.2.3 Estimation of the planetary boundary layer height

The Weather Research and Forecast model version 3.7.1 (www.wrf-model.org) (Skamarock et al., 2008) was used for this work. The WRF model initial and boundary conditions were derived from the US National Center for Environmental Prediction (NCEP)/National Center for Atmospheric Research (NCAR) Global Forecast System (GFS) at 1.0°×1.0° resolution (National Centers for Environmental Prediction, 2000), including Newtonian nudging every 6 hours. The Yonsei University Scheme (YSU) planetary boundary layer physics option was used here (Hong et al., 2006).

The WRF model domains setup used in this study had three nested domains with horizontal resolution of 0.5°×0.5° for the European domain, 0.16°×0.16° for the British Isles domain, and 0.055°×0.055° for the UK model domain. The vertical column was divided into 21 layers from the surface (bottom layer ~ 50 m) up to 100 hPa (~16 km) in sigma coordinates.

The WRF model hourly output from the UK domain was used to calculate a spatial average of the wind speed, wind direction, and the planetary boundary layer height. We estimate the spatial averages at a height of ~450 m (4th model layer) for an area defined as follow: lower left corner coordinates of 52.0 latitude and -10.0 longitude and the upper right corner of 57.0 latitude and 3.0 longitude. Time series of hourly averages of wind speed, wind direction and PBL height were constructed for the data period 01/01/2014 to 31/12/2017.

2.2.4 Mass balance calculations

The flux F_C of species C through a two-dimensional, vertical plane perpendicular to the mean wind direction can be expressed as (Cambaliza et al., 2014; White et al., 1976):

$$F_C = \int_{z_{min}}^{z_{max}} \int_{x_{min}}^{x_{max}} (C - C_b) \, . \, U_\perp \, dx \; dz \;, \tag{1}$$

In Eq. (1), C and C_b are the number of moles of species c downwind and upwind of the vertical plane, and $U_\perp$ is the mean wind speed perpendicular to the plane bounded horizontally by x_{min} and x_{max} and vertically by z_{min} and z_{max}.

F_c can be expressed explicitly in units of mol.s^{-1} as:

$$F_C = \int_{z_{ground}}^{z_{PBL}} \int_{x_{min}}^{x_{max}} \Delta\chi_C \, . \, U \, . \, n_{air}(z) \, . \, cos\theta \; dx \; dz \tag{2}$$

Here, $\Delta\chi_c$ is the enhancement of compound c in mol.mol^{-1} above background, $n_{air}(z)$ is the air density at height z, $cos\theta \, dx$ (Fig. 5) is the ship track increment projected onto the crosswind plane and U is the mean wind speed within the PBL obtained by the WRF-model described in Section 2.2.3.

In practice, despite the 3 years of data, no single journey satisfied all the quality control criteria detailed in Section 2.2.1 perfectly for all of the individual 5-minute averaging intervals and we opted to aggregate the good 5-minute data points into 0.2°- wide latitude bins using seasonal grouping for each data year. The baseline mole fractions used to calculate the upwind enhancement of compound c were time-shifted in order to account for the mean air mass travel time across the domain.

Seasonal budgets were then calculated from the aggregated data as:

$$F_C = \sum_{i=1}^{lat\ bins} \underbrace{\Delta x(i)}_{\equiv I} \, . \, \underbrace{\overline{\Delta\chi_C \, (\Delta t) . U(\Delta t) \, . \, cos(\theta(\Delta t)) \, . \int_{z_{ground}}^{z_{PBL}} n_{air}(\Delta t, z) dz}}_{\equiv II} \tag{3}$$

© Author(s) 2018. CC BY 4.0 License.

In Eq. (3), term *I* is the distance travelled per nominal latitude bin *i along a meridian* (the crosswind projection is done by multiplication with cos(θ) in term *II*) and term *II* is the mean (the horizontal bar denotes averaging), for latitude bin *i*, of the product over all the 5-minute averaging periods (Δt) that passed the quality control tests.

The total uncertainty on seasonal fluxes was approximated as:

$$\Delta F_c = \sqrt{\sum_{i=1}^{lat\ bins} \Delta x(i).\sigma^2 \left(\Delta\chi_C\ (\Delta t).U(\Delta t).cos\theta(\Delta t).\int_{z_{ground}}^{z_{PBL}} n_{air}(\Delta t, z)dz\right)} \quad (4)$$

where σ denotes the standard deviation of the mean. Finally, the annual budgets were obtained by summing the seasonal budgets.

3. Results

3.1 Seasonal and annual fluxes

The fluxes of CH_4 (Fig. 6) and CO_2 (Fig. 7) calculated from measurements on board the North Sea ferry were variable in space (over the latitude range 51.35° – 56.15° N) and time. The calculated emissions of CO_2 and CH_4 had maxima in winter (DJF; 379.1 ± 68.8 Tg CO_2, 0.89 ± 0.35 Tg CH_4; 2016 & 2017 winter data only). Emissions minima were observed in summer (JJA; 123.6 ± 64.6 Tg CO_2; 0.38 ± 0.09 Tg CH_4; Table 3). Springtime (MAM) emissions were 161.5 ± 41.2 Tg for CO_2 and 0.55 ± 0.17 Tg for CH_4 and, in autumn (SON), the measured emissions were 250.2 ± 57.8 Tg for CO_2 and 0.72 ± 0.16 Tg for CH_4. For CO_2, fluxes were statistically significantly different during winter compared with the other seasons, but for CH_4 a significant difference was found only between winter and summer. For both gases, the differences in emissions between spring and summer were not statistically significant, whilst, for autumn, they were only marginally significant. Annual budgets, estimated from seasonal values, were 914.4 ± 118.1 Tg for CO_2 and 2.55 ± 0.43 for CH_4. Without accounting for seasonality (i.e. using all data without seasonal segregation, which could weight towards the periods of the year for which the most data were available), the emissions budgets were 708.3 ± 241.9 Tg for CO_2 and 2.1 ± 0.63 for CH_4.

In winter, spring and autumn, the largest fluxes of both gases were found in a broad central latitudinal band (52 °N – 54 °N; Fig. 6 and Fig. 7). The lowest emissions were observed in summer across the entire spatial domain and they exhibited a smaller increment in the 52 °N – 54 °N band compared to the fringes of the domain than in other seasons.

3.2 Diurnal variability

There were differences between day (defined arbitrarily as 09:00 to 18:00) and night fluxes, particularly in spring and summer (Fig. 8, Fig. 9). Median daytime CO_2 fluxes were negative for latitudes in the range 54.5 °N to 55.9 °N in spring; in summer, negative CO_2 fluxes were found at 54.5 °N and 55.3 – 55.5 °N. It is important to note that air mass transit time between the in- and out-flow points of the domain varied from a median of 11 hours in winter to 19 hours in summer, which means that the day and night periods did overlap.

Seasonal and annual budgets were re-calculated using day and night fluxes weighted by day length (Table 3) in order to assess the impacts of uneven day/night data density distributions over the spatial domain caused by the relatively slow travel speed of the ship and the random data gaps introduced by changing wind direction and measurement downtime. The annual budgets calculated with day/night flux segregation were smaller than those obtained without day/night partitioning but the differences were not statistically significant and, in general, separating fluxes into day and night components increased the uncertainties on the final budgets both at the seasonal and annual levels.

© Author(s) 2018. CC BY 4.0 License.

The annual budgets calculated using all available data were smaller than those obtained from seasonal budgets (both with and without day/night segregation), however, the only statistically significant difference was between the annual budget of CO_2 obtained from seasonal data and the budget estimated with day/night weighting but without seasonality.

The annual budgets for both gases obtained without accounting for the seasonality in data coverage were consistent with inventory data but the measurement uncertainties were large (ranging from 30% to 57% for CH_4 with and without day/night weighting, with counterpart uncertainties on CO_2 budgets 34% and 46%, respectively). The annual budgets of CH_4 obtained from seasonal budgets were in good agreement with inventory data, with uncertainties of 17% and 19% for estimates calculated with and without day/night weighting, respectively. In contrast, CO_2 budgets were almost double the inventory value, with uncertainties of 13% and 16% for estimates calculated with and without day/night weighting.

The seasonal mass balance fluxes of CH_4 and CO_2 calculated from concentration measurements on the ferry were compared to known land sources and meteorological drivers of these gases. For both gases, there was a strong, positive correlation between seasonal emissions measured on the ferry and consumption of natural gas in the UK (Fig. 10). The correlation between GHG emissions and mean air temperature was negative and statistically significant (Fig. 11).

4. Discussion

The mass balance approach presented here relies on simplifying assumptions to derive GHG budgets for a large part of the British Isles. The main assumptions are that a) the air masses travel West to East, b) the PBL height is constant over the spatial domain for each nominal averaging period, c) there is no loss or input of mass into the domain other than from land sinks/ sources, and d) the air is well-mixed over the entire PBL height.

The data were filtered for westerly flow based on air mass back trajectories obtained from the HYSPLIT Trajectory model (NOAA Air Resources Laboratory, 2018) daily 72-hour runs at two coordinates: the Mace Head reference site and one ferry position halfway along its route. The back trajectories were run daily, commencing at midnight, and the air mass histories were assumed to be valid for an entire 24-hour period and for the entire spatial domain.

The fluxes calculated under this data filtering regime were assumed to be representative of surface emissions and uptake over the land masses bounded by the spatial domain and local influences (due to e.g. localised air re-circulation) were assumed to be negligible. This assumption could not be tested on a point-per-point basis but the latitudinal trends for both CH_4 and CO_2 at the seasonal time scale (Fig. 6 and Fig. 7) are consistent with the demographics and the known spatial distributions of sources of GHGs over the latitudinal range considered. In particular, the emission peaks for CO_2 observed around 52.5 °N and 54 °N coincide with major urbans centres in the British Midlands, namely Birmingham and Manchester/Liverpool/Leeds/Sheffield, and Dublin further upwind in the Republic of Ireland. These conurbations are reported to be significant sources of CO_2 by the UK's official National Atmospheric Emissions Inventory (NAEI, 2018a). The calculated CH_4 emissions were elevated in the 52.5 °N - 54 °N latitude band compared to the fringes of the domain. This agrees with the NAEI UK CH_4 map (NAEI, 2018a), which shows large emissions from the western parts of England in that latitude band. The NAEI reports substantial CH_4 emissions from the Cornwall area (SW England; latitudes < 51.3 °N), which might not always have registered in their entirety by the measurement system on the ferry because the port of Zeebrugge – the starting/end point of the vessel's route – lies at 51.21 °N.

The negative daytime fluxes of CO_2 registered in summer for latitudes > 54.5 °N are consistent with the demographics, topography and land-use of the northern parts of England and of Northern Ireland; these areas are less populated than the

© Author(s) 2018. CC BY 4.0 License.

southern parts, host the hills and mountains of the Lake District and the Northern Pennines and the land-use consists largely of grasslands. The combination of these factors (lower density of anthropogenic sources and higher density of biogenic sinks compared to southern parts of the UK) can explain the net negative fluxes of CO_2 measured during the daytime in spring and summer. Whilst the observed lower emissions of CO_2 in the northern parts of the spatial domain are consistent with the spatial distribution of emissions from NAEI data (NAEI, 2018a), Polson et al. (Polson et al., 2011) reported substantial summertime emissions from Ireland and Northern Ireland which should cancel out the sink terms in Northern England when integrating along a latitude bin. The fact that negative and very low summer emissions were derived by the ferry mass balance approach could indicate that measurements on board the ferry were more sensitive to sources and sinks in the eastern parts of the domain sampled because of, a) violation of the simplifying assumption that there is no loss of mass out of the domain, b) imperfect vertical mixing or, c) local air circulation which would not have been resolved by the HYSPLIT air mass histories. Alternatively, the mass balance estimates are real and the high CO_2 emissions assigned to Ireland in the aircraft inversion model are measurement artefacts caused by the venting of the nocturnal boundary layer as postulated by Polson et al. (Polson et al., 2011).

There was no statistically significant difference between day and night fluxes for CH_4, which could be because, a) the major sources of this gas in the British Isles (livestock - enteric fermentation and manure management - and waste treatment related emissions – landfills and waste water - 52.8% and 39.1% of the total CH_4 budget for the UK, respectively; BEIS, 2017) do not have marked diurnal cycles, b) the mass balance approach could not resolve them, c) the transit time of the air masses over the spatial domain blurred the potential differences between day and night time emissions or, c) the CH_4 signal measured on the ferry was contaminated and did not reflect emissions from the land surface. Due to the temporal and spatial averaging carried out to derive emission estimates from the ferry measurements, and due to the diffuse spatial distribution of the dominant land sources of CH_4, it seems likely that relatively small diurnal variations (e.g. studies indicate diurnal cycles in CH_4 emissions from dairy farms - (VanderZaag et al., 2014) - and from landfills sites - (Borjesson and Svensson, 1997)) would not be resolved by the mass balance approach.

At the seasonal time scale, the fluxes of CH_4 and CO_2 were both strongly correlated with UK natural gas usage (Fig. 10; BEIS, 2018); this provides confidence that the fluxes calculated by the mass balance approach can be related to physical emissions within the spatial domain and that the data filtering and quality control criteria excluded data points potentially contaminated by emissions from the ship. The statistically significant linear correlations between derived CH_4 and CO_2 fluxes and natural gas usage do not demonstrate causality, but suggest that the sources of these two GHGs within the domain sampled have seasonal dynamics similar to those of natural gas usage. However, both CH_4 and CO_2 emissions exhibited a weaker correlation with mean seasonal air temperature than with natural gas usage (Fig. 11), and this may indicate that natural gas consumption is a causal driver rather than a proxy for another underlying variable. Whilst it is reasonable to infer that both CO_2 and CH_4 would increase in line with an increasing demand for natural gas during the colder months, the NAEI (NAEI, 2018b) attributes only 15% of annual CH_4 emissions to fuel-related sources (combustion and fugitive emissions); this does not tally with the ~ 100% increase in CH_4 emissions between winter and summer which is accompanied by a similar increase in natural gas usage. An unexpectedly large diurnal and seasonal variability in the CH_4 flux was observed from direct flux measurements above London (Helfter et al., 2016) and this suggested that pressure variations in the gas supply network in respond to gas demand may have a significant impact on urban emissions. Fugitive emissions from the network may be underestimated in the NAEI.

Seasonality in methane emissions from landfills has also been reported, with higher emissions sometimes observed in winter and autumn (Borjesson and Svensson, 1997; Chanton and Liptay, 2000). The explanation for this is that net CH_4 emissions from landfill emissions can be largely regulated by methane oxidation in the top layer of the landfill cover soil: oxidation is limited by soil temperature and the methane-oxidising potential decreases in autumn and winter because of lower soil

© Author(s) 2018. CC BY 4.0 License.

temperatures, which results in an increase in methane emissions during the colder seasons. Riddick et al. (Riddick et al., 2017) reported a 71% winter-to-summer reduction in CH_4 emissions from a waste treatment park near Haddenham, England. Central England has the largest densities of waste treatment and landfill sites, which might explain the statistically significant, linear anti-correlation between seasonal CH_4 emissions and mean air temperature found in this region (Fig. 12). This is a remarkable result, which demonstrates the merit of this simple mass balance approach. In the other two regions considered ("N" and "S", i.e. north and south of the central region denoted as "MID"), there was no compelling correlation between CH_4 emissions and mean air temperature. This suggests that the dominant sources of this GHG in the N and S regions differ from the ones in the central region.

For CO_2, the seasonal emissions had statistically significant correlations to mean air temperature in the central and northern regions whilst the linear correlation was only marginally non-significant in the southern region. This is consistent with, a) the seasonality of natural gas usage (the NAEI attributes ~ 50% of annual CO_2 emissions to fuel combustion processes such as domestic and industrial gas usage; NAEI, 2018b) and, b) the seasonality of CO_2 uptake by vegetation.

Contrary to our findings, the UK CH_4 emissions derived by inverse modelling using concentration data from four tall tower sites distributed across the UK and Ireland did not exhibit any clear seasonality over the period August 2012 – August 2014 (Ganesan et al., 2015), but the range of emissions (1.65 Tg to 2.67 Tg) was consistent with the ferry measurements (1.52 ± 0.18 Tg to 3.56 ± 0.7 Tg).

For CH_4, all four annual budgets calculated using all the available data for the 2015-2017 period were consistent with the inventory values for the UK (excluding Scotland) and the Republic of Ireland, as well as with top-down modelling estimates (Table 3). Temporal data aggregation (i.e. not considering seasonality) increased the uncertainty on the final budget (30% and 57% uncertainty for annual budgets derived with and without considering differences in day and night emissions, compared to 17 % and 19% for the budgets where seasonality was factored in) and it seems therefore that this approach should be discarded. The difference between the annual CH_4 budgets calculated with and without day/night segregation but with seasonality was within the uncertainty of the individual estimates and since we found no compelling evidence of diurnal trends, we arrive at 2.55 ± 0.43 Tg y^{-1} as our final estimate of the methane emissions from the UK (excluding Scotland) and the Republic of Ireland for the period 2015-2017.

Following the same argument regarding temporal data aggregation, we derive an annual emission budget for CO_2 of 881.0 ± 137.5 Tg y^{-1}, which is the estimate obtained from seasonal budgets with day/night segregation because we found indications of diurnal trends in some parts of the spatial domain.

This value is over two-fold the inventory estimate of 422.7 Tg, but contrarily to CH_4, CO_2 has significant biogenic sources (e.g. the CO_2 exhaled by the 65 million-strong human population within the spatial domain considered is of the order of 18 Tg y^{-1} (Moriwaki and Kanda, 2004)) and sinks (vegetation uptake) which are not accounted for by the anthropogenic atmospheric emissions inventories; a direct comparison with the inventory is hence not possible. Polson et al. (2011) derived an annual budget for CO_2 of 620 ± 105 Tg y^{-1} from a series of flights around Britain in the summer of 2005 and September 2006. Using only summer data, in order to emulate the temporal upscaling done by Polson, we arrive at an annual CO_2 budget of 511 ± 157 Tg y^{-1}, which agrees with the 2011 aircraft study within measurement uncertainty. Whilst the seasonality of CO_2 emissions cannot be disregarded, comparing our summer time budgets with the aircraft study provides an independent validation of the ferry mass balance approach and gives us confidence in the method despite the simplifying assumptions that underpin it. Finally, we compared the ferry-derived summertime estimates for the southern region, filtered with a narrow 260°-280° wind direction window, to the fluxes of CO_2 and CH_4 obtained in 2012 by airborne measurements in the greater London area (O'Shea

© Author(s) 2018. CC BY 4.0 License.

et al., 2014). The ferry fluxes of both gases (CH_4: 0.049 ± 0.020 Tg.season^{-1}; CO_2: 24 ± 15 Tg.season^{-1}) compared reasonably well with the ones from the airborne campaign (CH_4: 0.034 ± 0.002 Tg.season^{-1}; CO_2: 13.4 ± 1.2 Tg.season^{-1}), but clearly also include sources upwind and downwind of the greater London area. The uncertainty was large for both gases, which is unsurprising considering the length of the averaging period (summers of 2015 and 2016), but this comparison with another independent measurement further consolidates the confidence in the method and in the overall annual budgets for CH_4 and CO_2.

5. Conclusions

Applying a mass balance approach to continuous measurements of CO_2 and CH_4 in the outflow, using a ship of opportunity, we estimated the net annual emissions of CH_4 from the UK (excluding Scotland) and the Republic of Ireland, averaged over the 2015-2017 period, to be 2.55 ± 0.43 Tg, which is consistent with the combined 2.29 Tg reported to the United Nations Framework Convention on Climate Change. The annual CO_2 budget obtained by mass balance (881.0 ± 137.5 Tg) was over two-fold the inventory value (422.7 Tg), but a direct comparison is not possible for this gas because the atmospheric inventory only accounts for anthropogenic sources. Instead we compared our CO_2 budget estimate with previous airborne studies, one for the UK as a whole and the second one for the greater London area and found good agreement with both. The mass balance approach presented here does not provide direct source apportionment information, but the latitudinal emissions patterns observed for both CH_4 and CO_2 were generally consistent with known spatial distributions of sources and sinks. Assuming that the atmospheric emissions inventory captures all anthropogenic emissions, we estimate that the net biogenic component of the measured CO_2 annual budget was 458.7 Tg, which corresponds to 52% of the total emissions. We detected marked seasonality in the emissions of both gases with lower values in the summer, and the seasonal budgets had statistically significant correlations with natural gas and mean air temperature. We attribute the two-thirds decrease in CO_2 emissions between winter and summer for CO_2 to the superposition of the reduction in demand for fossil fuels and an increase in the biogenic sink during the summer. For CH_4, we attribute the seasonal variability of the measured fluxes to natural gas consumption and to the waste management sector where temperature has been shown to control the methane oxidising potential of landfill cover soil and, thereby, the net emissions. With this study, we validated the atmospheric emissions inventory of CH_4 for the UK (excl. Scotland) and Ireland, quantified the biogenic component of the annual CO_2 budget and derived seasonal emissions budgets for both gases. Finally, we demonstrated that CH_4 emissions are strongly seasonal even at such a relatively large spatial scale, which highlights the importance of taking meteorological drivers such as air temperature into account in future "bottom-up" budgets.

Author contribution

Carole Helfter led the writing of the manuscript with contributions from all co-authors.

Acknowledgments

The GAUGE project was funded by the UK Natural Environment Research Council under grant reference NE/K002449/1.
We are grateful to DFDS Seaways for authorising the research activities on board the Rosyth–Zeebrugge commercial ferry and we thank the captains and crews of the Longstone (now the Finnmerchant) and Finlandia Seaways for access to the ships and for assistance with the day-to-day research operations. We also acknowledge the contributions of Gerry Spain (NUIG), Victor Kazan (LSCE) and Damien Martin (EPA, Ireland) for the maintenance of the analysers at the Mace Head measurement station.

© Author(s) 2018. CC BY 4.0 License.

References

Allen, G.: Rebalancing the global methane budget, Nature, 538, 46, 10.1038/538046a, 2016.

Bakwin, P. S., Tans, P. P., Zhao, C. L., Ussler, W., and Quesnell, E.: Measurements of carbon-dioxide on a very tall tower, Tellus Ser. B, 47, 535-549, 10.1034/j.1600-0889.47.issue5.2.x, 1995.

BEIS (Department for Business, Energy and Industrial Strategy): UK Greenhouse Gas Inventory, 1990 to 2015, in: Annual Report for Submission under the Framework Convention on Climate Change, Issue 2, available at: http://naei.beis.gov.uk/reports/reports?report_id=958 (last access 5 June 2018), 2017.

BEIS (Department for Business, Energy and Industrial Strategy): Natural Gas Supply and Consumption, Table ET 4.1, available at: https://www.gov.uk/government/statistics/gas-section-4-energy-trends (last access 5 June 2018), 2018.

Bergamaschi, P., Corazza, M., Karstens, U., Athanassiadou, M., Thompson, R. L., Pison, I., Manning, A. J., Bousquet, P., Segers, A., Vermeulen, A. T., Janssens-Maenhout, G., Schmidt, M., Ramonet, M., Meinhardt, F., Aalto, T., Haszpra, L., Moncrieff, J., Popa, M. E., Lowry, D., Steinbacher, M., Jordan, A., O'Doherty, S., Piacentino, S., and Dlugokencky, E.: Top-down estimates of European CH_4 and N_2O emissions based on four different inverse models, Atmos. Chem. Phys., 15, 715-736, 10.5194/acp-15-715-2015, 2015.

Biraud, S., Ciais, P., Ramonet, M., Simmonds, P., Kazan, V., Monfray, P., O'Doherty, S., Spain, T. G., and Jennings, S. G.: European greenhouse gas emissions estimated from continuous atmospheric measurements and radon 222 at Mace Head, Ireland, J. Geophys. Res.-Atmos., 105, 1351-1366, 10.1029/1999jd900821, 2000.

Bohnenstengel, S. I., Belcher, S. E., Aiken, A., Allan, J. D., Allen, G., Bacak, A., Bannan, T. J., Barlow, J. F., Beddows, D. C. S., Bloss, W. J., Booth, A. M., Chemel, C., Coceal, O., Di Marco, C. F., Dubey, M. K., Faloon, K. H., Fleming, Z. L., Furger, M., Gietl, J. K., Graves, R. R., Green, D. C., Grimmond, C. S. B., Halios, C. H., Hamilton, J. F., Harrison, R. M., Heal, M. R., Heard, D. E., Helfter, C., Herndon, S. C., Holmes, R. E., Hopkins, J. R., Jones, A. M., Kelly, F. J., Kotthaus, S., Langford, B., Lee, J. D., Leigh, R. J., Lewis, A. C., Lidster, R. T., Lopez-Hilfiker, F. D., McQuaid, J. B., Mohr, C., Monks, P. S., Nemitz, E., Ng, N. L., Percival, C. J., Prevot, A. S. H., Ricketts, H. M. A., Sokhi, R., Stone, D., Thornton, J. A., Tremper, A. H., Valach, A. C., Visser, S., Whalley, L. K., Williams, L. R., Xu, L., Young, D. E., and Zotter, P.: Meteorology, air quality, and health in London the ClearfLo project, B. Am. Meteorol. Soc., 96, 779-804, 10.1175/bams-d-12-00245.1, 2015.

Borjesson, G., and Svensson, B. H.: Seasonal and diurnal methane emissions from a landfill and their regulation by methane oxidation, Waste Manag. Res., 15, 33-54, 10.1177/0734242x9701500104, 1997.

Cambaliza, M. O. L., Shepson, P. B., Caulton, D. R., Stirm, B., Samarov, D., Gurney, K. R., Turnbull, J., Davis, K. J., Possolo, A., Karion, A., Sweeney, C., Moser, B., Hendricks, A., Lauvaux, T., Mays, K., Whetstone, J., Huang, J., Razlivanov, I., Miles, N. L., and Richardson, S. J.: Assessment of uncertainties of an aircraft-based mass balance approach for quantifying urban greenhouse gas emissions, Atmos. Chem. Phys., 14, 9029-9050, 10.5194/acp-14-9029-2014, 2014.

Cambaliza, M. O. L., Shepson, P. B., Bogner, J., Caulton, D. R., Stirm, B., Sweeney, C., Montzka, S. A., Gurney, K. R., Spokas, K., Salmon, O. E., Lavoie, T. N., Hendricks, A., Mays, K., Turnbull, J., Miller, B. R., Lauvaux, T., Davis, K., Karion, A., Moser, B., Miller, C., Obermeyer, C., Whetstone, J., Prasad, K., Miles, N., and Richardson, S.: Quantification and source

© Author(s) 2018. CC BY 4.0 License.

apportionment of the methane emission flux from the city of Indianapolis, Elementa-Science of the Anthropocene, 3, 10.12952/journal.elementa.000037, 2015.

Chanton, J., and Liptay, K.: Seasonal variation in methane oxidation in a landfill cover soil as determined by an in situ stable isotope technique, Glob. Biogeochem. Cycles, 14, 51-60, 10.1029/1999gb900087, 2000.

Dengel, S., Levy, P. E., Grace, J., Jones, S. K., and Skiba, U. M.: Methane emissions from sheep pasture, measured with an open-path eddy covariance system, Glob. Change Biol., 17, 3524-3533, 10.1111/j.1365-2486.2011.02466.x, 2011.

Derwent, R. G., Ryall, D. B., Manning, A., Simmonds, P. G., O'Doherty, S., Biraud, S., Ciais, P., Ramonet, M., and Jennings, S. G.: Continuous observations of carbon dioxide at Mace Head, Ireland from 1995 to 1999 and its net European ecosystem exchange, Atmos. Environ., 36, 2799-2807, 10.1016/s1352-2310(02)00203-0, 2002.

Dlugokencky, E. J., Nisbet, E. G., Fisher, R., and Lowry, D.: Global atmospheric methane: Budget, changes and dangers, Philos. Trans. Roy. Soc. A, 369, 2058-2072, 10.1098/rsta.2010.0341, 2011.

Erkkila, K.-M., Ojala, A., Bastviken, D., Biermann, T., Heiskanen, J. J., Lindroth, A., Peltola, O., Rantakari, M., Vesala, T., and Mammarella, I.: Methane and carbon dioxide fluxes over a lake: Comparison between eddy covariance, floating chambers and boundary layer method, Biogeosciences, 15, 429-445, 10.5194/bg-15-429-2018, 2018.

EPA (Environment Protection Agency): Ireland National Inventory Report 2017: Greenhouse Gas Emissions 1990-2015; available at: https://unfccc.int/process/transparency-and-reporting/reporting-and-review-under-the-convention/greenhouse-gas-inventories/submissions-of-annual-greenhouse-gas-inventories-for-2017 (last access 28 May 2018), 2017.

Felber, R., Muenger, A., Neftel, A., and Ammann, C.: Eddy covariance methane flux measurements over a grazed pasture: Effect of cows as moving point sources, Biogeosciences, 12, 3925-3940, 10.5194/bg-12-3925-2015, 2015.

Feng, L., Palmer, P. I., Bosch, H., and Dance, S.: Estimating surface CO_2 fluxes from space-borne CO_2 dry air mole fraction observations using an ensemble Kalman filter, Atmos. Chem. Phys., 9, 2619-2633, 10.5194/acp-9-2619-2009, 2009.

Feng, L., Palmer, P. I., Yang, Y., Yantosca, R. M., Kawa, S. R., Paris, J. D., Matsueda, H., and Machida, T.: Evaluating a 3-D transport model of atmospheric CO_2 using ground-based, aircraft, and space-borne data, Atmos. Chem. Phys., 11, 2789-2803, 10.5194/acp-11-2789-2011, 2011.

Fowler, D., Hargreaves, K. J., Choularton, T. W., Gallagher, M. W., Simpson, T., and Kaye, A.: Measurements of regional CH_4 emissions in the UK using boundary layer budget methods, Energy Conversion and Management, 37, 769-775, 10.1016/0196-8904(95)00254-5, 1996.

Gallagher, M. W., Choularton, T. W., Bower, K. N., Stromberg, I. M., Beswick, K. M., Fowler, D., and Hargreaves, K. J.: Measurements of methane fluxes on the landscape scale from a wetland area in north Scotland, Atmos. Environ., 28, 2421-2430, 10.1016/1352-2310(94)90394-8, 1994.

© Author(s) 2018. CC BY 4.0 License.

Ganesan, A. L., Manning, A. J., Grant, A., Young, D., Oram, D. E., Sturges, W. T., Moncrieff, J. B., and O'Doherty, S.: Quantifying methane and nitrous oxide emissions from the UK and Ireland using a national-scale monitoring network, Atmos. Chem. Phys., 15, 6393-6406, 10.5194/acp-15-6393-2015, 2015.

Gioli, B., Toscano, P., Lugato, E., Matese, A., Miglietta, F., Zaldei, A., and Vaccari, F. P.: Methane and carbon dioxide fluxes and source partitioning in urban areas: The case study of Florence, Italy, Environ. Pollut., 164, 125-131, 10.1016/j.envpol.2012.01.019, 2012.

Gregg, J. S., Andres, R. J., and Marland, G.: China: Emissions pattern of the world leader in CO_2 emissions from fossil fuel consumption and cement production, Geophys. Res. Lett., 35, 10.1029/2007gl032887, 2008.

Gregg, M.: Uncertainties in accounting for CO_2 from fossil fuels, J. Indust. Ecol., 12, 136-139, doi:10.1111/j.1530-9290.2008.00014.x, 2008.

Guan, D. B., Liu, Z., Geng, Y., Lindner, S., and Hubacek, K.: The gigatonne gap in China's carbon dioxide inventories, Nat. Clim. Chang., 2, 672-675, 10.1038/nclimate1560, 2012.

Hazan, L., Tarniewicz, J., Ramonet, M., Laurent, O. and Abbaris, A., Automatic processing of atmospheric CO_2 and CH_4 mole fractions at the ICOS Atmosphere Thematic Centre, Atmos. Meas. Tech., 9, 4719–4736, 10.5194/amt-9-4719-2016, 2016.

Helfter, C., Famulari, D., Phillips, G. J., Barlow, J. F., Wood, C. R., Grimmond, C. S. B., and Nemitz, E.: Controls of carbon dioxide concentrations and fluxes above central London, Atmos. Chem. Phys., 11, 1913-1928, 10.5194/acp-11-1913-2011, 2011.

Helfter, C., Tremper, A. H., Halios, C. H., Kotthaus, S., Bjorkegren, A., Grimmond, C. S. B., Barlow, J. F., and Nemitz, E.: Spatial and temporal variability of urban fluxes of methane, carbon monoxide and carbon dioxide above London, UK, Atmos. Chem. Phys., 16, 10543-10557, 10.5194/acp-16-10543-2016, 2016.

Hiller, R. V., Neininger, B., Brunner, D., Gerbig, C., Bretscher, D., Kuenzle, T., Buchmann, N., and Eugster, W.: Aircraft-based CH_4 flux estimates for validation of emissions from an agriculturally dominated area in Switzerland, J. Geophys. Res.-Atmospheres, 119, 4874-4887, 10.1002/2013jd020918, 2014.

Hong, S.-Y., Noh, Y., and Dudhia, J.: A New Vertical Diffusion Package with an Explicit Treatment of Entrainment Processes, Mon. Weather Rev., 134, 2318-2341, 10.1175/mwr3199.1, 2006.

IPCC (International Panel on Climate Change): 2006 IPCC Guidelines for National Greenhouse Gas Inventories, available at https://www.ipcc-nggip.iges.or.jp/public/2006gl/vol1.html (last access 12 June 2018), 2006.

Karion, A., Sweeney, C., Petron, G., Frost, G., Hardesty, R. M., Kofler, J., Miller, B. R., Newberger, T., Wolter, S., Banta, R., Brewer, A., Dlugokencky, E., Lang, P., Montzka, S. A., Schnell, R., Tans, P., Trainer, M., Zamora, R., and Conley, S.: Methane emissions estimate from airborne measurements over a Western United States natural gas field, Geophys. Res. Lett., 40, 4393-4397, 10.1002/grl.50811, 2013.

© Author(s) 2018. CC BY 4.0 License.

Karion, A., Sweeney, C., Kort, E. A., Shepson, P. B., Brewer, A., Cambaliza, M., Conley, S. A., Davis, K., Deng, A. J., Hardesty, M., Herndon, S. C., Lauvaux, T., Lavoie, T., Lyon, D., Newberger, T., Petron, G., Rella, C., Smith, M., Wolter, S., Yacovitch, T. I., and Tans, P.: Aircraft-based estimate of total methane emissions from the Barnett shale region, Environ. Sci. Technol., 49, 8124-8131, 10.1021/acs.est.5b00217, 2015.

Kirschke, S., Bousquet, P., Ciais, P., Saunois, M., Canadell, J. G., Dlugokencky, E. J., Bergamaschi, P., Bergmann, D., Blake, D. R., Bruhwiler, L., Cameron-Smith, P., Castaldi, S., Chevallier, F., Feng, L., Fraser, A., Heimann, M., Hodson, E. L., Houweling, S., Josse, B., Fraser, P. J., Krummel, P. B., Lamarque, J.-F., Langenfelds, R. L., Le Quéré, C., Naik, V., O'Doherty, S., Palmer, P. I., Pison, I., Plummer, D., Poulter, B., Prinn, R. G., Rigby, M., Ringeval, B., Santini, M., Schmidt, M., Shindell, D. T., Simpson, I. J., Spahni, R., Steele, L. P., Strode, S. A., Sudo, K., Szopa, S., van der Werf, G. R., Voulgarakis, A., van Weele, M., Weiss, R. F., Williams, J. E., and Zeng, G.: Three decades of global methane sources and sinks, Nat. Geosci., 6, 813, 10.1038/ngeo1955, 2013.

Marland, G.: Emissions accounting China's uncertain CO_2 emissions, Nat. Clim. Chang., 2, 645-646, 10.1038/nclimate1670, 2012.

Mays, K. L., Shepson, P. B., Stirm, B. H., Karion, A., Sweeney, C., and Gurney, K. R.: Aircraft-based measurements of the carbon footprint of Indianapolis, Environ. Sci. Technol., 43, 7816-7823, 10.1021/es901326b, 2009.

Meijide, A., Manca, G., Goded, I., Magliulo, V., di Tommasi, P., Seufert, G., and Cescatti, A.: Seasonal trends and environmental controls of methane emissions in a rice paddy field in northern Italy, Biogeosciences, 8, 3809-3821, 10.5194/bg-8-3809-2011, 2011.

Met Éireann: Meteorological data from Mace Head station obtained at: http://www.met.ie/climate-request/ (last access 30 march 2018). Met Éireann Data is licensed under a Creative Commons Attribution-ShareAlike 4.0 International Licence, 2018. Met Office: UK and Regional Series obtained at: https://www.metoffice.gov.uk/climate/uk/summaries/datasets (last access 5 June 2018). UK Open Government Licence for Public Sector Information v3.0 @ Crown Copyright 2018.

Miller, S. M., Wofsy, S. C., Michalak, A. M., Kort, E. A., Andrews, A. E., Biraud, S. C., Dlugokencky, E. J., Eluszkiewicz, J., Fischer, M. L., Janssens-Maenhout, G., Miller, B. R., Miller, J. B., Montzka, S. A., Nehrkorn, T., and Sweeney, C.: Anthropogenic emissions of methane in the United States, Proc. Natl. Acad. Sci. U.S.A., 110, 20018-20022, 10.1073/pnas.1314392110, 2013.

Moriwaki, R., and Kanda, M.: Seasonal and diurnal fluxes of radiation, heat, water vapor, and carbon dioxide over a suburban area, J. Appl. Meteorol., 43, 1700-1710, 10.1175/jam2153.1, 2004.

NAEI (National Atmospheric Emissions Inventory): UK Emissions Interactive Maps, available at: http://naei.beis.gov.uk/data/gis-mapping (last access 8 August 2018), 2018a.

NAEI (National Atmospheric Emissions Inventory): Greenhouse gas inventories for England, Scotland, Wales & Northern Ireland: 1990-2016, available at: http://naei.beis.gov.uk/reports/reports?report_id=958 (last access 12 June 2018), 2018b.

© Author(s) 2018. CC BY 4.0 License.

National Centers for Environmental Prediction/National Weather Service/NOAA/U.S. Department of Commerce (2000), NCEP FNL Operational Model Global Tropospheric Analyses, continuing from July 1999, https://doi.org/10.5065/D6M043C6, Research Data Archive at the National Center for Atmospheric Research, Computational and Information Systems Laboratory, Boulder, Colo. (Updated daily.) Accessed 01 Jan 2017, 2000.

Nicolini, G., Castaldi, S., Fratini, G., and Valentini, R.: A literature overview of micrometeorological CH_4 and N_2O flux measurements in terrestrial ecosystems, Atmos. Environ., 81, 311-319, 10.1016/j.atmosenv.2013.09.030, 2013.

Nisbet, E., and Weiss, R.: Top-down versus bottom-up, Science, 328, 1241-1243, 10.1126/science.1189936, 2010.

NOAA Air Resources Laboratory: HYSPLIT trajectory model, available at: https://www.ready.noaa.gov/HYSPLIT.php (last access 9 September 2018), 2018.

Oney, B., Henne, S., Gruber, N., Leuenberger, M., Bamberger, I., Eugster, W., and Brunner, D.: The Carbocount CH sites: Characterization of a dense greenhouse gas observation network, Atmos. Chem. Phys., 15, 11147-11164, 10.5194/acp-15-11147-2015, 2015.

O'Shea, S. J., Allen, G., Fleming, Z. L., Bauguitte, S. J. B., Percival, C. J., Gallagher, M. W., Lee, J., Helfter, C., and Nemitz, E.: Area fluxes of carbon dioxide, methane, and carbon monoxide derived from airborne measurements around Greater London: A case study during summer 2012, J. Geophys. Res. Atmos., 119, 4940-4952, 10.1002/2013jd021269, 2014.

Palmer, P. I., O'Doherty, S., Allen, G., Bower, K., Bösch, H., Chipperfield, M. P., Connors, S., Dhomse, S., Feng, L., Finch, D. P., Gallagher, M. W., Gloor, E., Gonzi, S., Harris, N. R. P., Helfter, C., Humpage, N., Kerridge, B., Knappett, D., Jones, R. L., Le Breton, M., Lunt, M. F., Manning, A. J., Matthiesen, S., Muller, J. B. A., Mullinger, N., Nemiitz, E., O'Shea, S., Parker, R. J., Percival, C. J., Pitt, J., Riddick, S. N., Rigby, M., Sembhi, H., Siddans, R., Skelton, R. L., Smith, P., Sonderfeld, H., Stanley, K., Stavert, A. R., Wenger, A., White, E., Wilson, C., and Young, D.: A measurement-based verification framework for UK greenhouse gas emissions: An overview of the Greenhouse gAs Uk and Global Emissions (GAUGE) project, Atmos. Chem. Phys., 18, 11753–11777, 10.5194/acp-18-11753-2018, 2018.

Pawlak, W., and Fortuniak, K.: Eddy covariance measurements of the net turbulent methane flux in the city centre - results of 2-year campaign in Łódź, Poland, Atmos. Chem. Phys., 16, 8281-8294, 10.5194/acp-16-8281-2016, 2016.

Pawlak, W., Fortuniak, K., Siedlecki, M., and Zielinski, M.: Urban - wetland contrast in turbulent exchange of methane, Atmos. Environ., 145, 176-191, 10.1016/j.atmosenv.2016.09.036, 2016.

Peltola, O., Hensen, A., Helfter, C., Marchesini, L. B., Bosveld, F. C., van den Bulk, W. C. M., Elbers, J. A., Haapanala, S., Holst, J., Laurila, T., Lindroth, A., Nemitz, E., Rockmann, T., Vermeulen, A. T., and Mammarella, I.: Evaluating the performance of commonly used gas analysers for methane eddy covariance flux measurements: The InGOS inter-comparison field experiment, Biogeosciences, 11, 3163-3186, 10.5194/bg-11-3163-2014, 2014.

Peltola, O., Hensen, A., Marchesini, L. B., Helfter, C., Bosveld, F. C., van den Bulk, W. C. M., Haapanala, S., van Huissteden, J., Laurila, T., Lindroth, A., Nemitz, E., Rockmann, T., Vermeulen, A. T., and Mammarella, I.: Studying the spatial variability

© Author(s) 2018. CC BY 4.0 License.

of methane flux with five eddy covariance towers of varying height, Agric. For. Meteorol., 214, 456-472, 10.1016/j.agrformet.2015.09.007, 2015.

Peters, G. P., Marland, G., Le Quéré, C., Boden, T., Canadell, J. G., and Raupach, M. R.: Rapid growth in CO_2 emissions after the 2008–2009 global financial crisis, Nat. Clim. Chang., 2, 2, 10.1038/nclimate1332, 2011.

Podgrajsek, E., Sahlee, E., and Rutgersson, A.: Diurnal cycle of lake methane flux, J. Geophys. Res.: Biogeosci., 119, 236-248, 10.1002/2013jg002327, 2014.

Polson, D., Fowler, D., Nemitz, E., Skiba, U., McDonald, A., Famulari, D., Di Marco, C., Simmons, I., Weston, K., Purvis, R., Coe, H., Manning, A. J., Webster, H., Harrison, M., O'Sullivan, D., Reeves, C., and Oram, D.: Estimation of spatial apportionment of greenhouse gas emissions for the UK using boundary layer measurements and inverse modelling technique, Atmos. Environ., 45, 1042-1049, 10.1016/j.atmosenv.2010.10.011, 2011.

Ramonet, M., Ciais, P., Aalto, T., Aulagnier, C., Chevallier, F., Cipriano, D., Conway, T. J., Haszpra, L., Kazan, V., Meinhardt, F., Paris, J. D., Schmidt, M., Simmonds, P., Xueref-Remy, I., and Necki, J. N.: A recent build-up of atmospheric CO_2 over Europe. Part 1: Observed signals and possible explanations, Tellus B, 62, 1-13, 10.1111/j.1600-0889.2009.00442.x, 2010.

Riddick, S. N., Connors, S., Robinson, A. D., Manning, A. J., Jones, P. S. D., Lowry, D., Nisbet, E., Skelton, R. L., Allen, G., Pitt, J., and Harris, N. R. P.: Estimating the size of a methane emission point source at different scales: From local to landscape, Atmos. Chem. Phys., 17, 7839-7851, 10.5194/acp-17-7839-2017, 2017.

Rigby, M., Prinn, R. G., Fraser, P. J., Simmonds, P. G., Langenfelds, R. L., Huang, J., Cunnold, D. M., Steele, L. P., Krummel, P. B., Weiss, R. F., O'Doherty, S., Salameh, P. K., Wang, H. J., Harth, C. M., Muehle, J., and Porter, L. W.: Renewed growth of atmospheric methane, Geophys. Res. Lett., 35, 10.1029/2008gl036037, 2008.

Saunois, M., Bousquet, P., Poulter, B., Peregon, A., Ciais, P., Canadell, J. G., Dlugokencky, E. J., Etiope, G., Bastviken, D., Houweling, S., Janssens-Maenhout, G., Tubiello, F. N., Castaldi, S., Jackson, R. B., Alexe, M., Arora, V. K., Beerling, D. J., Bergamaschi, P., Blake, D. R., Brailsford, G., Brovkin, V., Bruhwiler, L., Crevoisier, C., Crill, P., Covey, K., Curry, C., Frankenberg, C., Gedney, N., Hoeglund-Isaksson, L., Ishizawa, M., Ito, A., Joos, F., Kim, H.-S., Kleinen, T., Krummel, P., Lamarque, J.-F., Langenfelds, R., Locatelli, R., Machida, T., Maksyutov, S., McDonald, K. C., Marshall, J., Melton, J. R., Morino, I., Naik, V., O'Doherty, S., Parmentier, F.-J. W., Patra, P. K., Peng, C., Peng, S., Peters, G. P., Pison, I., Prigent, C., Prinn, R., Ramonet, M., Riley, W. J., Saito, M., Santini, M., Schroeder, R., Simpson, I. J., Spahni, R., Steele, P., Takizawa, A., Thornton, B. F., Tian, H., Tohjima, Y., Viovy, N., Voulgarakis, A., van Weele, M., van der Werf, G. R., Weiss, R., Wiedinmyer, C., Wilton, D. J., Wiltshire, A., Worthy, D., Wunch, D., Xu, X., Yoshida, Y., Zhang, B., Zhang, Z., and Zhu, Q.: The global methane budget 2000-2012, Earth Sys. Sci. Data, 8, 697-751, 10.5194/essd-8-697-2016, 2016.

Schwietzke, S., Sherwood, O. A., Bruhwiler, L. M. P., Miller, J. B., Etiope, G., Dlugokencky, E. J., Michel, S. E., Arling, V. A., Vaughn, B. H., White, J. W. C., and Tans, P. P.: Upward revision of global fossil fuel methane emissions based on isotope database, Nature, 538, 88, 10.1038/nature19797, 2016.

Skamarock, W., Klemp, J., Dudhia, J., Gill, D., Barker, D., Duda, M., Huang, X.-Y., Wang, W., and J., P.: A description of the advanced research WRF version 3, NCAR Technical Note, NCAR/TN-475+STR, Colorado,2008.

© Author(s) 2018. CC BY 4.0 License.

Stanley, K. M., Grant, A., O'Doherty, S., Young, D., Manning, A. J., Stavert, A. R., Spain, T. G., Salameh, P. K., Harth, C. M., Simmonds, P. G., Sturges, W. T., Oram, D. E., and Derwent, R. G.: Greenhouse gas measurements from a UK network of tall towers: Technical description and first results, Atmos. Meas. Tech., 11, 1437-1458, 10.5194/amt-11-1437-2018, 2018.

Stavert, A. R., O'Doherty, S., Stanley, K., Young, D., Manning, A. J., Lunt, M. F., Rennick, C., and Arnold, T.: UK greenhouse gas measurements at two new tall towers for aiding emissions verification, Atmos. Meas. Tech. Discuss., 2018, 1-55, 10.5194/amt-2018-140, 2018.

UNFCCC (United Nations Framework Convention on Climate Change): Report of the Conference of The Parties on its Nineteenth Session, Held in Warsaw from 11 to 23 November 2013, available at: https://unfccc.int/resource/docs/2013/cop19/eng/10a03.pdf#page=2 (last access 5 June 2018), 2014.

Van der Zaag, A. C., Flesch, T. K., Desjardins, R. L., Balde, H., and Wright, T.: Measuring methane emissions from two dairy farms: Seasonal and manure-management effects, Agric. For. Meteorol., 194, 259-267, 10.1016/j.agrformet.2014.02.003, 2014.

White, W. H., Anderson, J. A., Blumenthal, D. L., Husar, R. B., Gillani, N. V., Husar, J. D., and Wilson, W. E.: Formation and transport of secondary air-pollutants - ozone and aerosols in St-Louis urban plume, Science, 194, 187-189, 10.1126/science.959846, 1976.

Atmos. Chem. Phys. Discuss., https://doi.org/10.5194/acp-2018-948
Manuscript under review for journal Atmos. Chem. Phys.
Discussion started: 1 October 2018
© Author(s) 2018. CC BY 4.0 License.

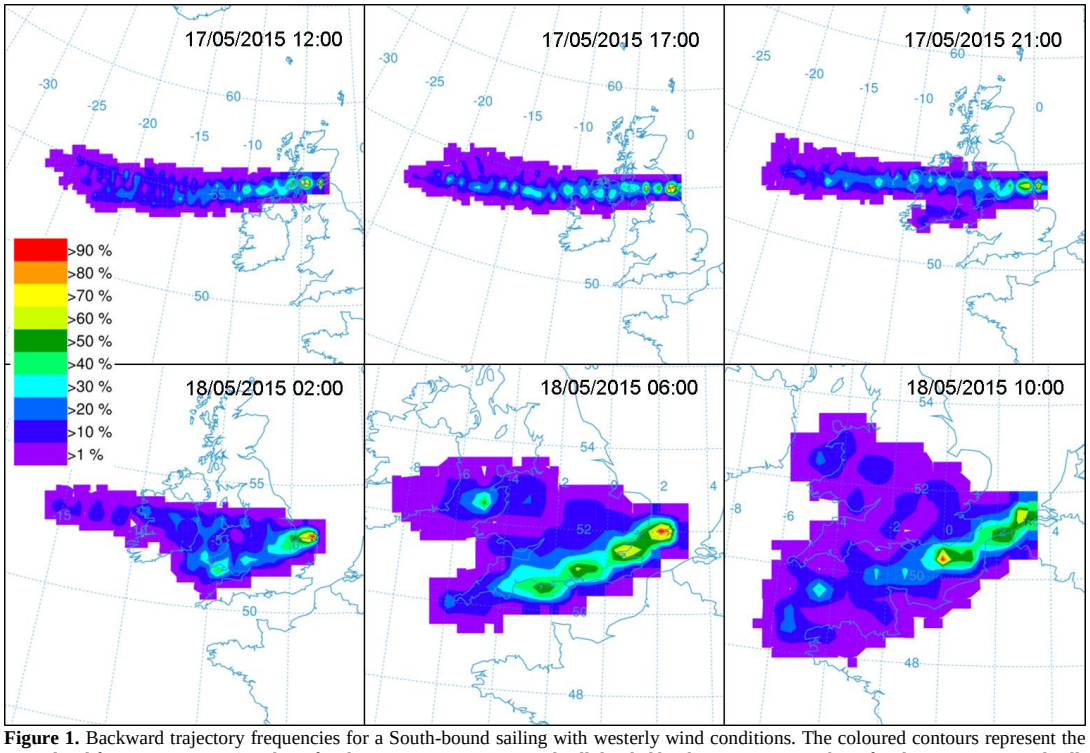

Figure 1. Backward trajectory frequencies for a South-bound sailing with westerly wind conditions. The coloured contours represent the normalised frequency counts (number of end points in a 0.5°x 0.5° grid cell divided by the maximum number of end points in any grid cell, expressed as a percentage) and the source corresponds to the location of the ferry. The trajectories were run backward for 24 hours at 3-hour intervals using GDAS 1-degree global meteorology (NOAA, 2018).

Atmos. Chem. Phys. Discuss., https://doi.org/10.5194/acp-2018-948
Manuscript under review for journal Atmos. Chem. Phys.
Discussion started: 1 October 2018
© Author(s) 2018. CC BY 4.0 License.

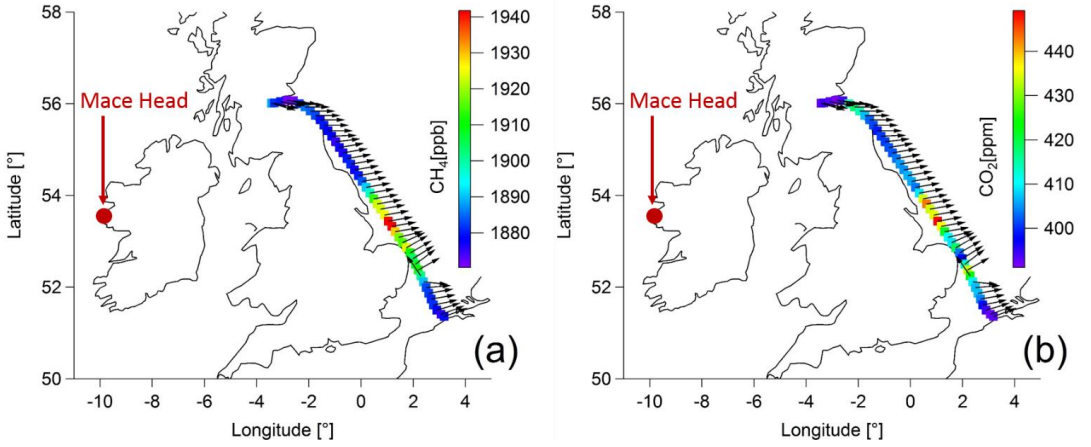

Figure 2. Half-hourly averages of (a) CH_4 and (b) CO_2 mole fractions measured on board the freight ferry during the South-bound journey on 29-30 July 2014. The arrows represent wind direction.

Atmos. Chem. Phys. Discuss., https://doi.org/10.5194/acp-2018-948
Manuscript under review for journal Atmos. Chem. Phys.
Discussion started: 1 October 2018
© Author(s) 2018. CC BY 4.0 License.

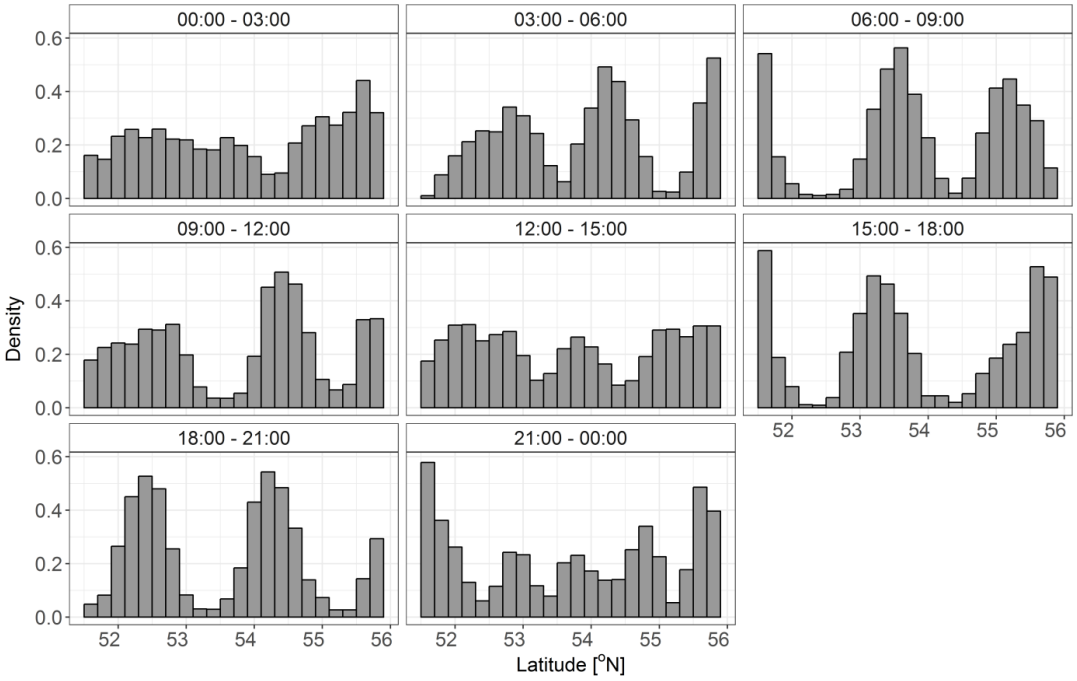

Figure 3. Temporal coverage of the latitudinal range (0.2° bins) spanned by the ferry route expressed as a counts density (frequency of occurrence normalised by the total number of observations in each latitude bin) for all data points which satisfied the data screening criteria (section 2.2.1) during the measurement period 01/01/2015 – 31/12/2017.

Atmos. Chem. Phys. Discuss., https://doi.org/10.5194/acp-2018-948
Manuscript under review for journal Atmos. Chem. Phys.
Discussion started: 1 October 2018
© Author(s) 2018. CC BY 4.0 License.

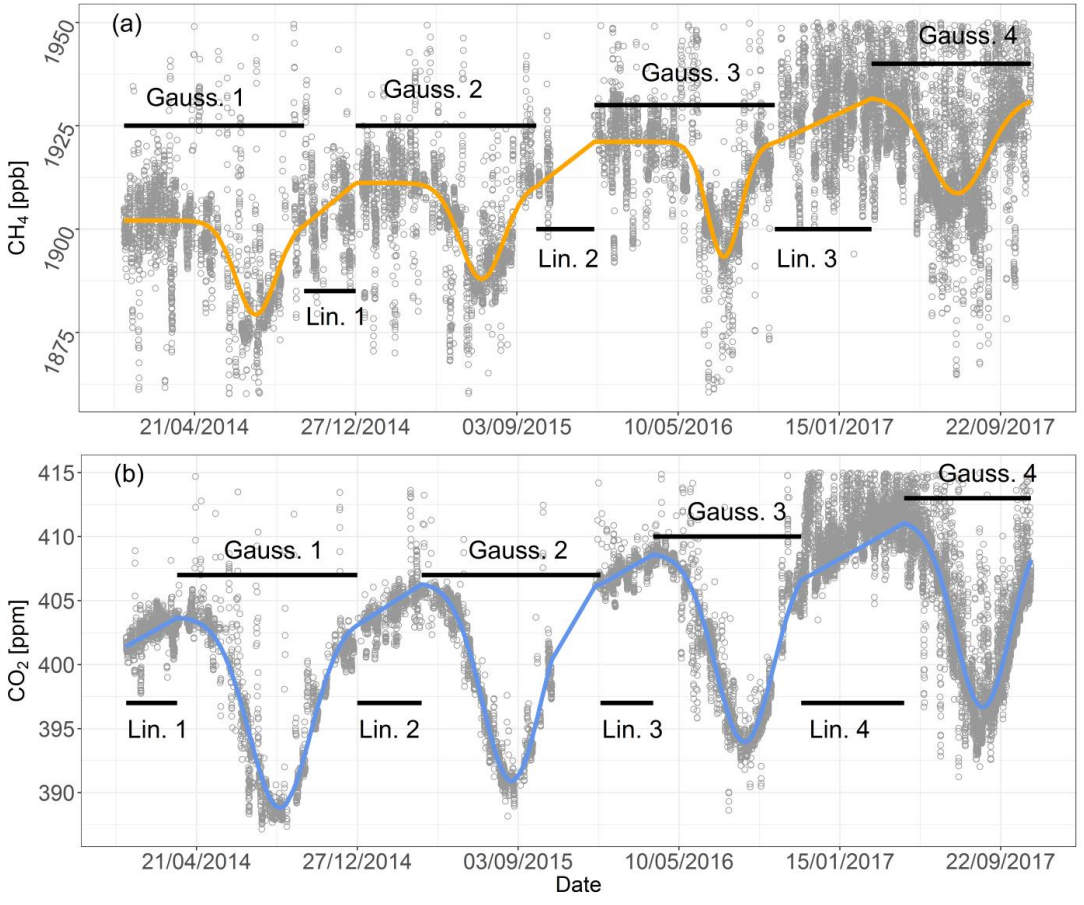

Figure 4. Hourly time series filtered for Westerly wind directions (range 150° – 210°) measured at the Mace Head station (open circles) of (a) CH_4 and (b) CO_2 mole fractions. Smoothing and gap filling of the original time series was achieved by applying linear (Lin.) and non-linear (Gauss.) regressions by parts for the data period 01/01/2014 – 31/12/2017 (solid lines).

Atmos. Chem. Phys. Discuss., https://doi.org/10.5194/acp-2018-948
Manuscript under review for journal Atmos. Chem. Phys.
Discussion started: 1 October 2018
© Author(s) 2018. CC BY 4.0 License.

Atmospheric Chemistry and Physics Discussions

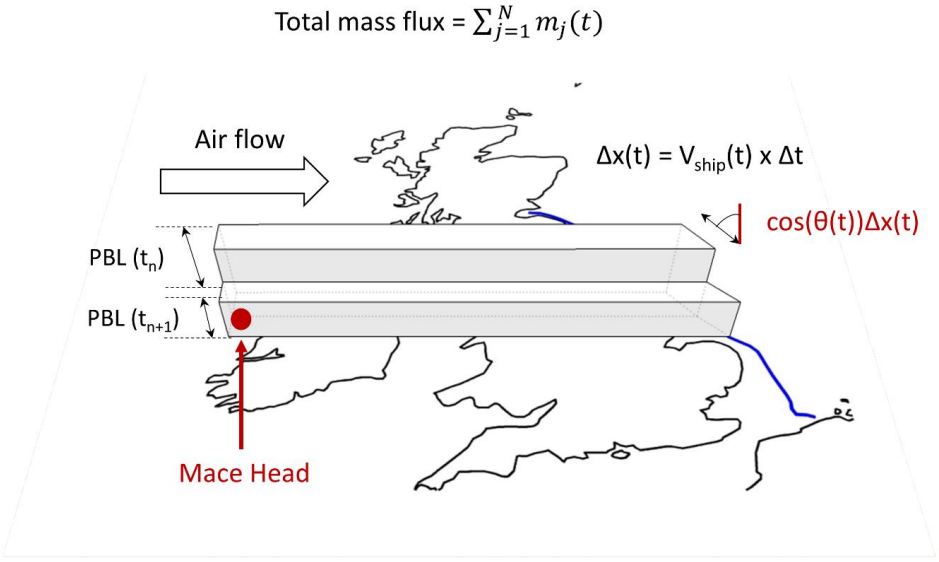

Figure 5. Schematic of the mass balance flux calculation procedure expressed in Eq. (2). The total flux is the sum of flux elements through a vertical surface of height that of the planetary boundary layer (PBL) height and width the ship track increment ($\Delta x = v_{ship}(t)\ \Delta t$) during a nominal averaging time interval Δt projected onto the cross-wind direction ($\cos((\theta(t))\ \Delta x$).

5

Atmos. Chem. Phys. Discuss., https://doi.org/10.5194/acp-2018-948
Manuscript under review for journal Atmos. Chem. Phys.
Discussion started: 1 October 2018
© Author(s) 2018. CC BY 4.0 License.

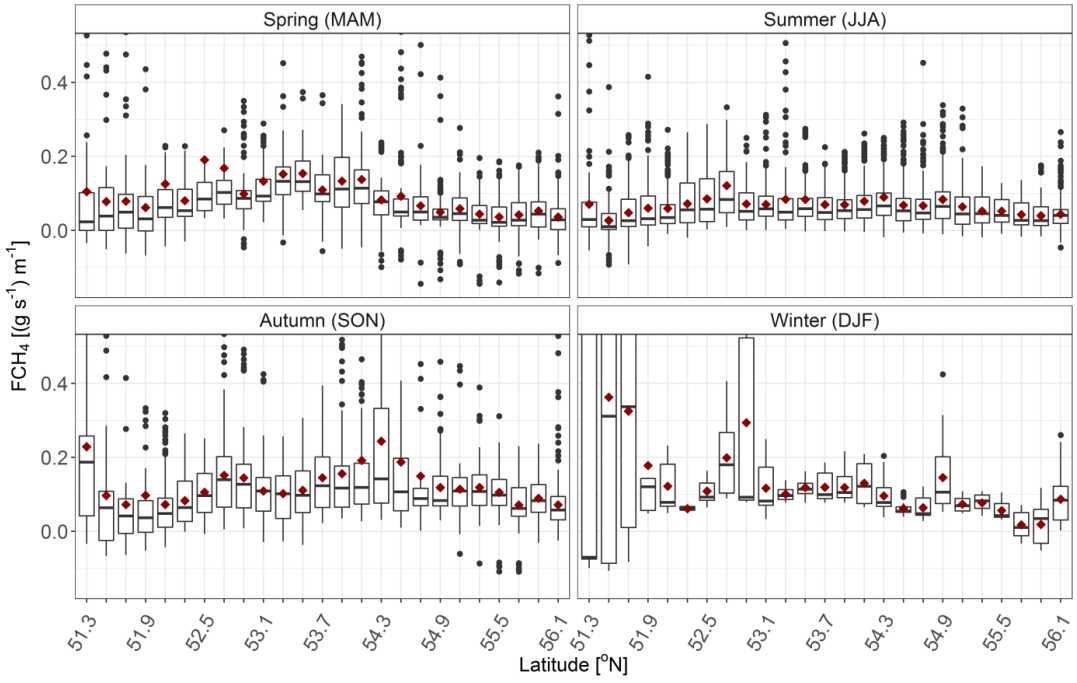

Figure 6. Box and whisker plots of 5-minute binned averages of CH_4 fluxes along the route of the ferry (latitude bin width: 0.2°). The horizontal bar within each box corresponds to the median for a given latitude bin, the upper and lower hinges represent the 75th and 25th quantiles, respectively, and the upper and lower whiskers indicate the largest/smallest observation less/greater than or equal to upper/lower hinge +/- 1.5 * IQR (Inter-Quantile Range), respectively. The outliers are represented by solid circles and arithmetic means by red diamonds. The flux is integrated over the height of the planetary boundary layer and expressed in units of mass flux per meter travelled crosswind within each latitude bin per unit time.

Atmos. Chem. Phys. Discuss., https://doi.org/10.5194/acp-2018-948
Manuscript under review for journal Atmos. Chem. Phys.
Discussion started: 1 October 2018
© Author(s) 2018. CC BY 4.0 License.

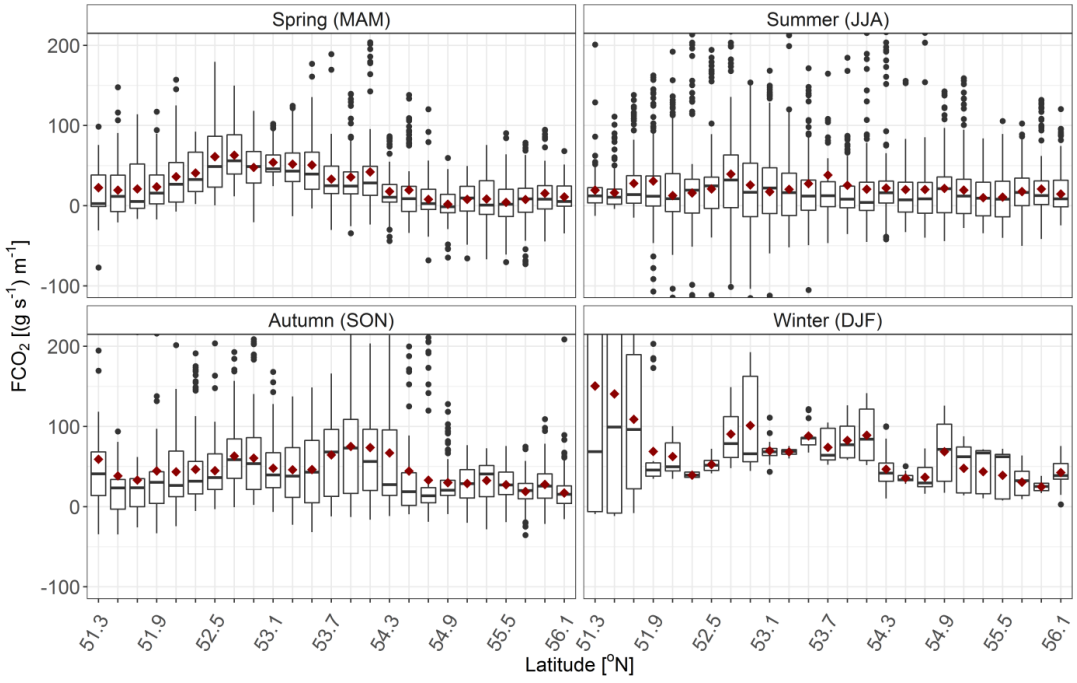

Figure 7. Box and whisker plots of 5-minute binned averages of CO_2 fluxes along the route of the ferry (latitude bin width: 0.2°). The horizontal bar within each box corresponds to the median for a given latitude bin, the upper and lower hinges represent the 75th and 25th quantiles, respectively, and the upper and lower whiskers indicate the largest/smallest observation less/greater than or equal to upper/lower hinge +/- 1.5 * IQR (Inter-Quantile Range), respectively. The outliers are represented by solid circles and arithmetic means by red diamonds. The flux is integrated over the height of the planetary boundary layer and expressed in units of mass flux per meter travelled crosswind within each latitude bin per unit time.

Atmos. Chem. Phys. Discuss., https://doi.org/10.5194/acp-2018-948
Manuscript under review for journal Atmos. Chem. Phys.
Discussion started: 1 October 2018
© Author(s) 2018. CC BY 4.0 License.

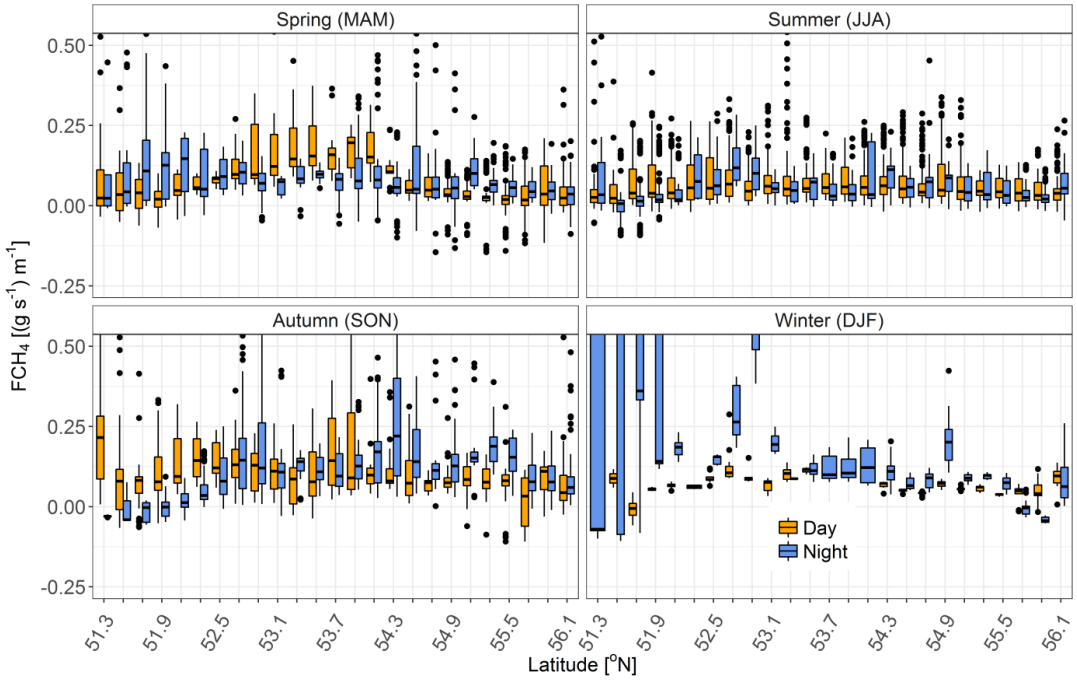

Figure 8. Box and whisker plots of 5-minute binned averages of CH_4 fluxes along the route of the ferry (latitude bin width: 0.2°) segregated into day and night contributions. The horizontal bar within each box corresponds to the median for a given latitude bin, the upper and lower hinges represent the 75th and 25th quantiles, respectively, and the upper and lower whiskers indicate the largest/smallest observation less/greater than or equal to upper/lower hinge +/- 1.5 * IQR (Inter-Quantile Range), respectively. The outliers are represented by solid circles and arithmetic means by red diamonds. The flux is integrated over the height of the planetary boundary layer and expressed in units of mass flux per meter travelled crosswind within each latitude bin per unit time.

Atmos. Chem. Phys. Discuss., https://doi.org/10.5194/acp-2018-948
Manuscript under review for journal Atmos. Chem. Phys.
Discussion started: 1 October 2018
© Author(s) 2018. CC BY 4.0 License.

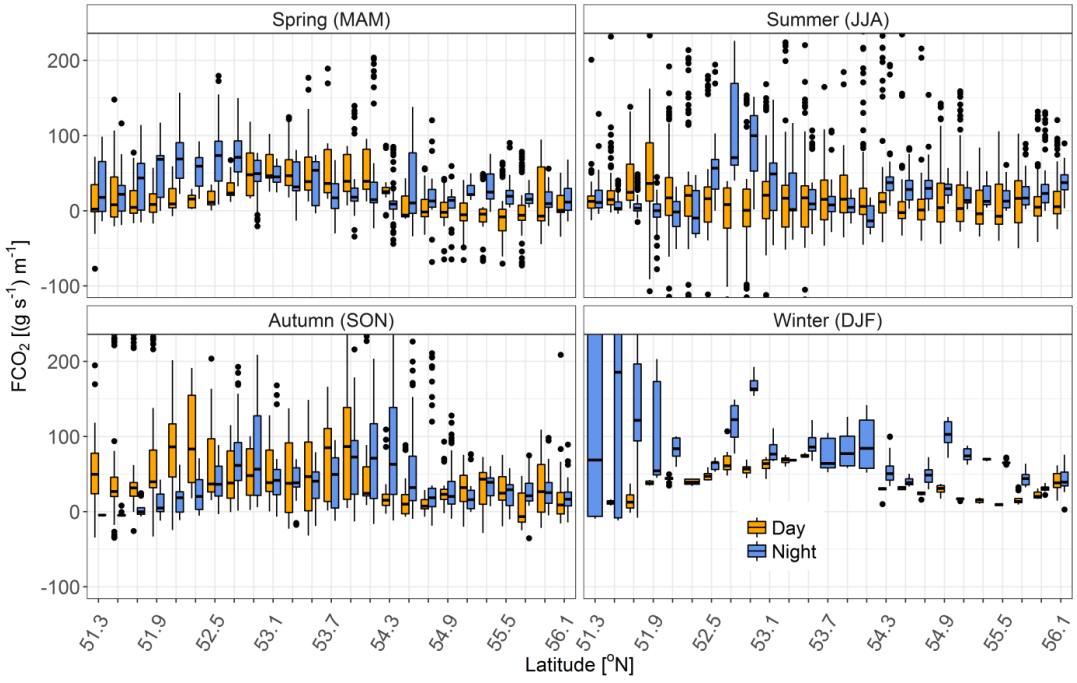

Figure 9. Box and whisker plots of 5-minute binned averages of CO_2 fluxes along the route of the ferry (latitude bin width: 0.2°) segregated into day and night contributions. The horizontal bar within each box corresponds to the median for a given latitude bin, the upper and lower hinges represent the 75th and 25th quantiles, respectively, and the upper and lower whiskers indicate the largest/smallest observation less/greater than or equal to upper/lower hinge +/- 1.5 * IQR (Inter-Quantile Range), respectively. The outliers are represented by solid circles and arithmetic means by red diamonds. The flux is integrated over the height of the planetary boundary layer and expressed in units of mass flux per meter travelled crosswind within each latitude bin per unit time.

Atmos. Chem. Phys. Discuss., https://doi.org/10.5194/acp-2018-948
Manuscript under review for journal Atmos. Chem. Phys.
Discussion started: 1 October 2018
© Author(s) 2018. CC BY 4.0 License.

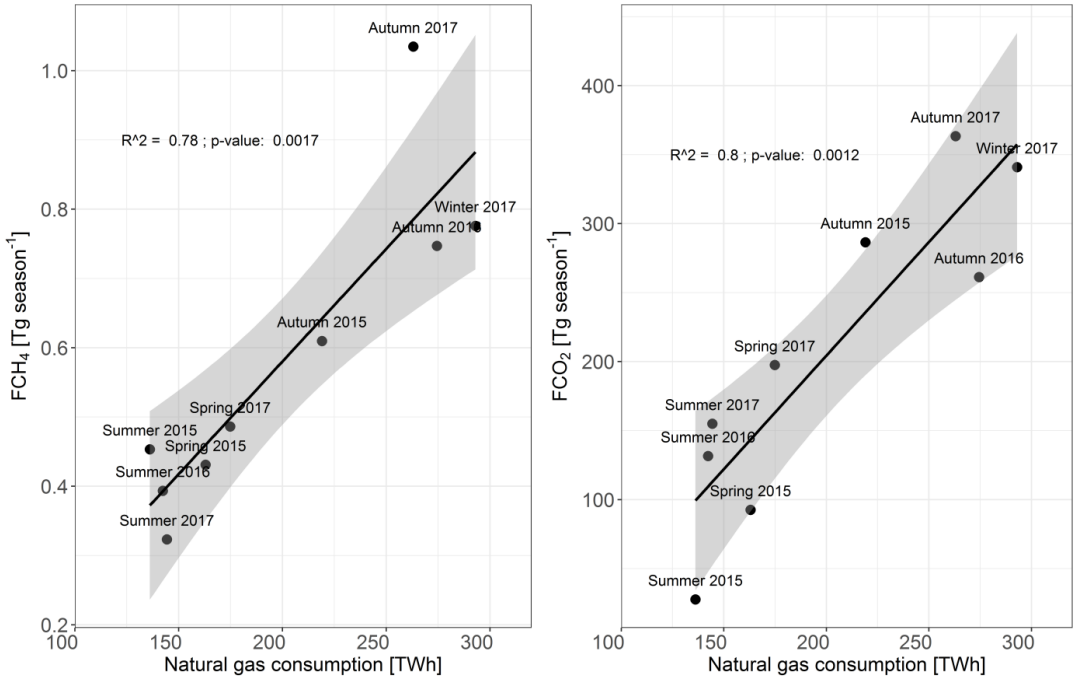

Figure 10. Seasonal budgets of CH_4 and CO_2 as function of UK natural gas consumption (source: BEIS, 2018).

Atmos. Chem. Phys. Discuss., https://doi.org/10.5194/acp-2018-948
Manuscript under review for journal Atmos. Chem. Phys.
Discussion started: 1 October 2018
© Author(s) 2018. CC BY 4.0 License.

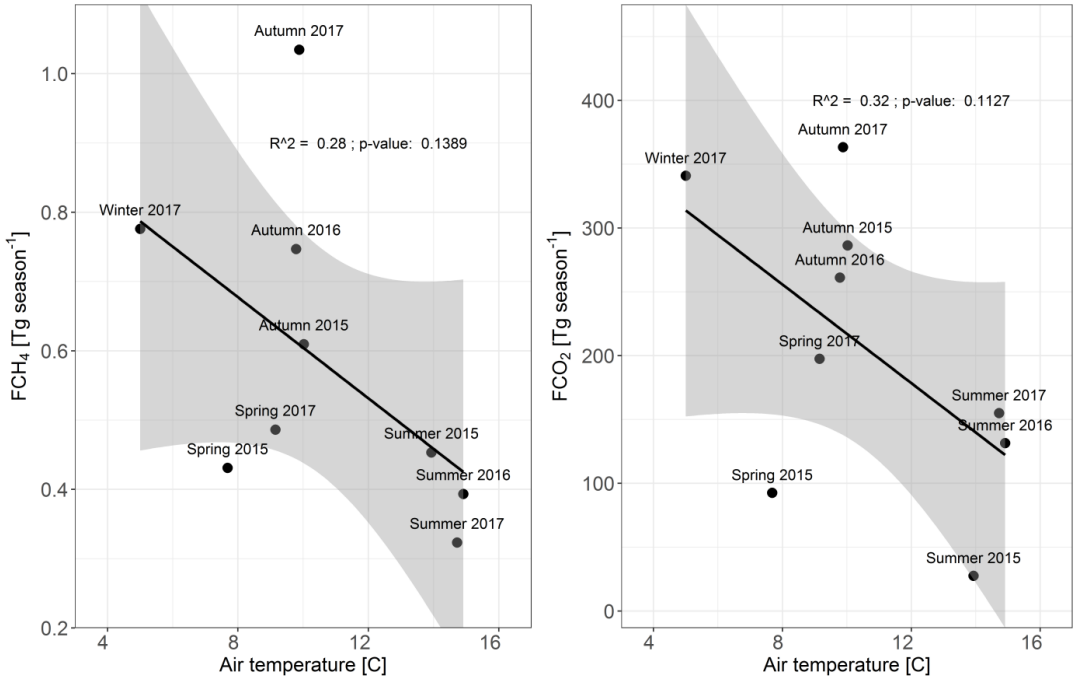

Figure 11. Seasonal budgets of CH_4 and CO_2 as function of mean UK air temperature (source: Met Office, 2018).

Atmos. Chem. Phys. Discuss., https://doi.org/10.5194/acp-2018-948
Manuscript under review for journal Atmos. Chem. Phys.
Discussion started: 1 October 2018
© Author(s) 2018. CC BY 4.0 License.

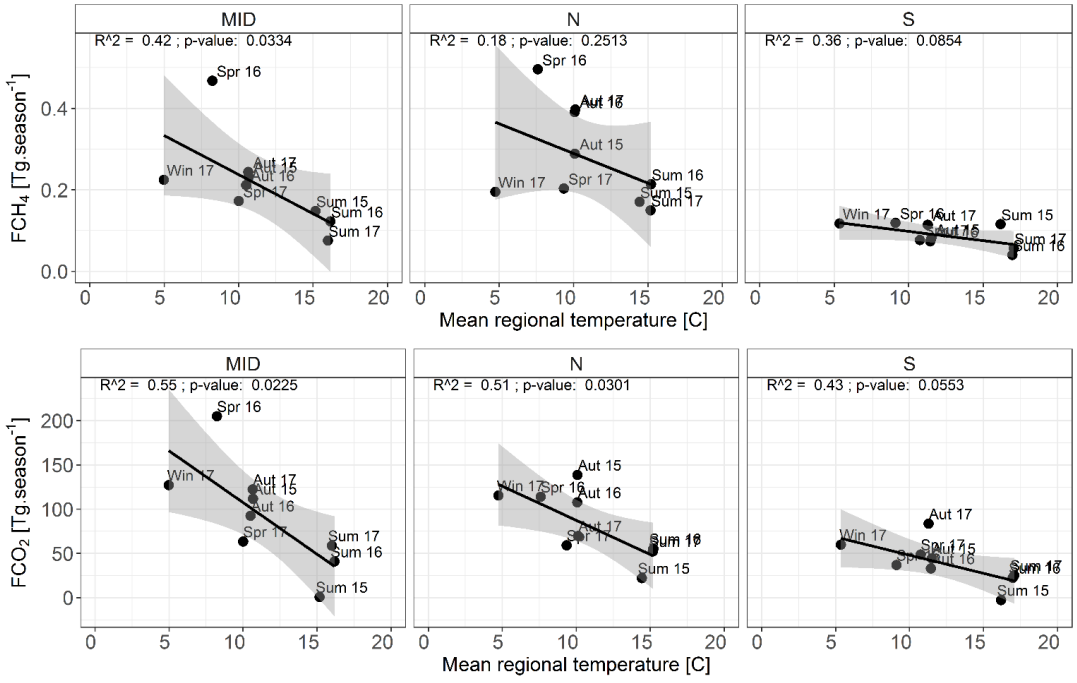

Figure 12. Seasonal fluxes of CH_4 and CO_2 estimated by mass balance from concentration measurements on board the ferry as function of mean UK air temperature. The data are presented for three latitudinal regions denoted "MID", "N" and "S". The "MID" region spans the latitude range 52.8 °N – 54.2 °N, "N" spans 54.2 °N – 56.1 °N and "S" spans 52.0 °N – 52.8 °N.

Atmos. Chem. Phys. Discuss., https://doi.org/10.5194/acp-2018-948
Manuscript under review for journal Atmos. Chem. Phys.
Discussion started: 1 October 2018
© Author(s) 2018. CC BY 4.0 License.

Atmospheric Chemistry and Physics Discussions

Table 1. List of instruments and observables recorded on board the Rosyth (Scotland, UK; 56° 1' 21.611'' N, 3° 26' 21.558'' W) to Zeebrugge (Belgium; 51° 21' 16.96'' N, 3° 10' 34.645'' E) freight ferry.

Observable	Unit	Instrument
CO_2 dry mole fraction	ppm	Picarro 1301 CRDS
CH_4 dry mole fraction	ppb	Picarro 1301 CRDS
Apparent wind speed (with respect to moving ship)	$m.s^{-1}$	Vaisala WXT520
Apparent wind direction (wind blowing from with respect to prow of moving ship)	degrees	Vaisala WXT520
Air temperature	°C	Vaisala WXT520
Ambient pressure	hPa	Vaisala WXT520
Relative humidity	%	Vaisala WXT520
Ship speed	kt	Garmin 18x series GPS
Ship bearing	degrees	Garmin 18x series GPS
Ship position, latitude	decimal	Garmin 18x series GPS
Ship position, longitude	decimal	Garmin 18x series GPS

Atmos. Chem. Phys. Discuss., https://doi.org/10.5194/acp-2018-948
Manuscript under review for journal Atmos. Chem. Phys.
Discussion started: 1 October 2018
© Author(s) 2018. CC BY 4.0 License.

Atmospheric Chemistry and Physics Discussions

Table 2. Details of the weekly auto-calibration sequence (interval 169 hours) and reference gases. The references gases were calibrated by the Swiss Federal Laboratories for Materials Testing and Research (EMPA, Dübendorf, Switzerland) using a Picarro 1301 CRDS. Calibrations scales (NOAA/ ESRL): WMO-CH_4-X2004 for methane and WMO-CO_2-X2007 for carbon dioxide. The measurement uncertainties correspond to the standard uncertainty multiplied by a coverage factor k = 2.

Step	**Type**	**Time interval [s]**	**CO_2 ± uncertainty [ppm]**	**CH_4 ± uncertainty [ppb]**
1	Purge	300		
2	Measurement	900	384.23 ± 0.15	1815.36 ± 1.45
3	Purge	300		
4	Measurement	900	418.29 ± 0.16	2018.06 ± 1.58
5	Purge	300		
6	Measurement	900	474.86 ± 0.18	2426.77 ± 1.86
7	Purge	300	Ambient air	Ambient air

© Author(s) 2018. CC BY 4.0 License.

Table 3. Seasonal and annual budgets for CO_2 and CH_4 for the United Kingdom (excluding Scotland) and Ireland estimated by a mass balance approach using concentrations measured at the Mace Head station (Republic of Ireland; 53° 19' 19.2'' N, 9° 54' 3.599'' W) and on board the freight ferry which serves the Rosyth (Scotland, UK; 56° 1' 21.611'' N, 3° 26' 21.558'' W) to Zeebrugge (Belgium; 51° 21' 16.96'' N, 3° 10' 34.645'' E) route. Seasonal budgets were calculated by year – where sufficient data was available; seasonal budgets were also derived using the entire dataset with and without segregation of the raw fluxes into day and night components. Annual budgets were calculated with and without seasonality and with and without day/night segregation.

Season	Year	Flux ± uncertainty [Tg]	
		CO_2	CH_4
Winter	2015	-	-
Spring	2015	92.6 ± 34.7	0.43 ± 0.11
Summer	2015	27.6 ± 46.8	0.45 ± 0.09
Autumn	2015	286.4 ± 47.6	0.61 ± 0.14
Winter	2016	-	-
Spring	2016	-	-
Summer	2016	131.6 ± 36.5	0.39 ± 0.09
Autumn	2016	261.3 ± 56.4	0.75 ± 0.16
Winter	2017	341 ± 62.1	0.78 ± 0.38
Spring	2017	197.5 ± 27.9	0.49 ± 0.07
Summer	2017	155 ± 77.6	0.32 ± 0.06
Autumn	2017	363.4 ± 65.7	1.03 ± 0.15
Winter	2016 & 2017	379.1 ± 68.8	0.89 ± 0.35
Spring	2015 – 2017	161.5 ± 41.2	0.55 ± 0.17
Summer	2015 – 2017	123.6 ± 64.6	0.38 ± 0.09
Autumn	2015 – 2017	250.2 ± 57.8	0.72 ± 0.16
Winter (day/night weighting)	2016 & 2017	357.8 ± 66.8	0.82 ± 0.34
Spring (day/night weighting)	2015 – 2017	162.5 ± 55.0	0.57 ± 0.22
Summer (day/night weighting)	2015 – 2017	127.7 ± 78.7	0.39 ± 0.12
Autumn (day/night weighting)	2015 – 2017	232.9 ± 72.2	0.67 ± 0.19
Annual (from seasonal budgets)	2015 – 2017	914.4 ± 118.1	2.55 ± 0.43
Annual (from seasonal, day/night weighted budgets)	2015 – 2017	881.0 ± 137.5	2.44 ± 0.47
Annual (no seasons)	2015 – 2017	708.3 ± 241.9	2.1 ± 0.63
Annual (no seasons, day/night weighted)	2015 – 2017	598.3 ± 274.9	1.66 ± 0.94
UK (Department for Business, 2017)	2015	415.1	2.1

© Author(s) 2018. CC BY 4.0 License.

RoI (Agency, 2017)	2015	38.4	0.53
Scotland (Inventory, 2018)	2015	30.8	0.34
Total inventory (UK – Scotland + RoI)	2015	422.7	2.29
Ganesan (Ganesan et al., 2015)	2012 - 2014	-	1.65 - 2.67
Bergamaschi (Bergamaschi et al., 2015)	2006 - 2007	-	3.1 – 3.5